Reply to Joe Todd

This study combines multiple observational records with inverse modelling to study the ice dynamics, stress & fracture of the Brunt Ice Shelf. Data from satellites & in situ measurements are assimilated into the SSA model Úa to invert for the flow parameter A across the shelf, and the resulting stress maps are analysed to build up a timeline of ice shelf stress conditions before, during and after the re-activation of Chasm 1 and the propagation of the Halloween crack. This is an interesting and well-presented study which warrants publication in The Cryosphere; as the authors note, the 'natural' cycle of stress concentration and release on ice shelves is a major factor controlling calving. I strongly agree with the conclusion that full-thickness rifting should be resolved in ice-sheet models. I think the manuscript could benefit from some additional details on the modelling results and some clarifications.

Thank you for these positive comments.

General comments:
It is not totally clear from the figure captions & text whether the stress maps shown in Figs. 2 & 3 come from Úa model output. I can see 3 possibilities: (1) The stress maps are produced using observed velocity (from which strain can be derived) and an assumed constant flow parameter A. (2) As above, but A comes from Úa output. (3) The stress maps are a direct output of Úa simulations. The text strongly implies (3) but, from reading the methods section, I do not think that any fractured domains were studied with the model. Is rifting accounted for through inversions (i.e. low A where rifts exist)? If (3) is the case, more details should be added to explain how the rifting is accounted for. If (3) is not the case, clarifications and modifications are required in the text to avoid giving a false impression to the reader. It would be nice to see the results of the model inversion (maps of 'A') and this would probably also help clarify the point above. In general, it's just not very clear at present exactly *how* the model was used.

Snapshots of observed surface velocities and ice shelf geometries were assimilated into Úa, and for each snapshot, an optimal solution for *A* was obtained through an inverse method, which optimizes the misfit between observed and modelled surface velocities. The resulting solutions for *A* together with the diagnostic surface velocities were used to calculate the stress maps. We have clarified our methodology in section 3, and added further details about the inverse method and resulting maps of *A* in Appendix A. To address your concern about the absence/inclusion of fractures in the domain, we also provided a comparison for *A* and the stress field between (1) the inversion with a continuous mesh (i.e., rifts are filled with ice/melange), and (2) the inversion with rifts as holes in the mesh (i.e., rifts correspond to open ocean) in Appendix B. In summary, method (1) produces high values of *A* along the trajectory of active rifts, whereas in method (2) these high values are absent. Yet, the derived large-scale stress distribution of the ice shelf remains qualitatively similar between both methods, which demonstrates the robustness of our results with respect to the representation of rifts in the model domain.

Specific Comments:

1

P3L9-10 – Can the broad-scale pattern of ice shelf thinning be established? Paolo et al. (2015) seem to provide data which covers the BIS. You make a compelling argument for the first-order importance of internal dynamics/heterogeneity for crack propagation, but does this completely preclude any external environmental signal?

We have no additional data on broad-scale changes in ice thickness other than the maps produced by Paolo et al.. This work was cited in the paper.

P4L3: This sentence implies that all the stress results shown in the paper are Ua model output. Is that the case?

All stress maps were calculated from diagnostic model output, i.e., an optimal solution for A and corresponding surface velocities for different snapshots in time. 'Optimal' is defined in the sense of inverse theory, i.e. as a minimum of the cost function which penalizes the difference between (gradients of) the observed and modelled surface velocities (see Appendix A for further details).

P4L8: Could you show the inverted-for A parameter, perhaps in supplementary material? Presumably there are some pretty interesting patterns.

More details about the model inversion and patterns for A are included in Appendix A.

P5L3-11: I am not totally clear what the approach is here. How do you shift the DEM to an effective timestamp? What does the LIDAR data provide?

Both points have been further clarified in the text.

P6L14: Again, this strongly implies that Fig 2 & 3 represent model output.

The calculation of the stress field requires the surface velocities in combination with a rheological model. As a first approximation, the rheology A can be assumed to be spatially constant and observed velocities can be used to calculate the stress field. However, a more accurate approach is to allow for a spatially variable A (obtained through a formal inversion of the observed surface velocities) and use the corresponding modelled surface velocities. In the latter approach, which was followed here, the forward model can be interpreted as a physically-based filter to reduce the measurement noise. These points have been clarified in section 3.

P6L26: 'Ocean pressure acting on newly formed rift surfaces' - I'm slightly confused by this. On a floating shelf, the overall ocean pressure should be equal to the hryostatic pressure which existed before the crack formed. The exception, which I guess applies here, is if the intact shelf was under significant tension. But is it really accurate that the ocean pressure is pushing the rift apart? I'd have thought that its the concentration of the supported stresses onto a narrower band (the remaining intact ice) which promotes further fracture growth.

We did not mean to imply that ocean pressure drives rift propagation, rather to emphasize the importance of normal pressure acting on newly formed surfaces for the force balance. Note however that perturbation experiments by Gudmundsson et al. 2017 have shown that if the ice melange inside Chasm 1 is removed and replaced by a normal ocean boundary condition, changes to the flow of the ice shelf remain small compared to the 2-fold increase in flow speed since 2012. To avoid confusion, we have reformulated this paragraph.

Fig 1 or 2: As I was reading the results section, I was thinking it'd be nice to clearly visualise the compressive arch. Could you perhaps add a panel (or overlay Fig 1a) showing regions with extension in both directions, versus one compressional component (like Doake et al., 1998).

In the interest of keeping the figures as simple as possible, we had hoped that the reader would be able to approximately trace the outlines of the compressive arch from the arrows in Figure 2, as black arrows are extensive and red arrows are compressive.

Fig 4b: Observations & model match well to the south of the MIR, but the difference grows further north. Can you speculate why?

The key process that causes a slow-down of the ice shelf is the regrounding of the MIR, which is represented well in the model. Further away from the MIR, where the impact of regrounding becomes weaker, other factors come into play, such as temporal changes in the rheology or damage, which are not represented in the model (this has been further clarified in section 6). In particular, further towards the east, just outside the limits of the figure, lies another active rift called the Brunt-StancombWills rift (see e.g. [Gudmundsson et al., 2017]) that locally affects the observed velocities.

Minor Comments:
P2L27: A bit pedantic, but I think 'single' would be better than 'singular' here. 'Singular' tends to refer to an exceptional event or thing.

We have removed 'singular' from the text

P3L15: 'preconditions for rifting were re-established'. What were these preconditions? I think the rest of the paper lays out what these preconditions were, but its perhaps a little premature to say this here without explanation.

We added '(as will be explained in section 4)'

P3L18: 'singular' again

We have removed 'singular' from the text

3

P4L11: slight formatting error – ref in brackets

Brackets have been removed.

Fig 1: North arrow?

As we plotted parallels and meridians (dashed grey lines) in figure 1, we did not see the need to include a north arrow.

Fig 2: Unless is really reduces the clarity of the figures, I'd think that for a colour scale with a white minimum, the minimum ought to be 0 kPa.

In this figure we draw the reader's attention to spatial patterns, with most of the relevant variability between 40 and 130kPa, as reflected in the colour scale. We did not see any benefit in colouring areas with background stresses below 40kPa, as these do not contribute to the story.

Reply to Jeremy Bassis

1   Overarching comments

This study describes a comparison between observations and model inferred stresses for the Brunt ice shelf. The authors demonstrate that the collision of the Brunt ice shelf with a pinning point resulted in increased compressive and tensile stresses and argue that this resulted in the increased tensile stresses needed to reactivate rift propagation. Overall, the results are highly glaciologically relevant and add to our understanding of ice shelf rift propagation.

Thank you for these kind words, and for your in-depth review, which –we believe- has led to important improvements in the presentation of our results.

The manuscript does feel a little bit like it was originally intended for a short form journal with a restrictive length requirement and has not taken advantage of the more generous space allocated by longer form journals. As such, I had a hard time understanding what was actually done and it seemed as though there were critical details missing from the exposition. Without those details it is hard to assess the reliability of the methods and conclusions drawn. There are also a few places in the manuscript where the text does not appear to accurately reflect the literature or conclusions are not fully supported by the results. My review is relatively long, but most of the issues are (hopefully) easy to correct by expanding the text to include more critical information.

We have expanded the manuscript, in particular the data and methods section, to clarify your points of concern and provide the critical details that were missing. Two appendices were added with additional

4

information about the modelling approach, including details about the inversion method, treatment of the rifts (see below for further comments), and examples of the inferred rate factors.

2 Major Comments:

The most significant issue in the manuscript relates to how the authors define a "rift" in the model and how this compares to how the rift actually behaves. We know that rifts in ice shelves can be discontinuities in the ice (fractures) that are filled with ocean water. Rifts are also often filled with a mixture of snow, sea ice and blocks of ice called melange. The melange can become structurally coherent to the point that rifts are barely visible on the surface of the ice, although this tends to be more common in relic rifts that have not been active for decades (or even centuries). Rifts can be represented in models in different ways. The most physically consistent way is to incorporate rifts as actual discontinuities in the ice shelf (see Larour et al., 2014). One then needs to account for the thickness of melange that fills rifts when applying a normal traction boundary condition along the rift walls, analogous to the calving front boundary condition. Historically, rifts have also been represented in models as regions of intact ice with a rate factor that is set (or inferred) to be much lower than is traditional for intact ice. In this representation, rifts not discontinuities and these features essentially behave like diffuse zones of really warm ice and NOT as fractures. The authors need to be clear about how rifts are represented in their model before any inferences can be made about the effect of "rifts" on the dynamics of ice shelves.

We agree that our *diagnostic* estimates of maximal principal stress, based on snapshots of observed ice velocity, ice thickness and an inferred rate factor (using inverse methods), are not obviously independent of the computational mesh. As you point out, a continuous mesh with soft ice filling the rifts or a mesh with holes might produce a different stress balance. We discuss this issue in Appendix B. As expected, inversions for a continuous mesh produce high values of the rate factor along the trajectory of active rifts (Figure B1, top left panel), whereas for the mesh with holes, these high values are absent (Figure B1, top right panel). However, the derived large-scale stress distribution of the ice shelf remains qualitatively similar between both cases (Figure B1, bottom panels). This is perhaps not surprising as the stresses are strongly controlled by the strain rates, which are forced to be identical for both meshes, by nature of the inverse method.
On the other hand, results from *transient* simulations in section 6 do not include any rift dynamics and we did not address the important question of how active rifts are treated in a transient run – mesh splitting, ice softening, … We have clarified this point in section 6.

A second, and closely related point, arises from circularity in tuning a model to fit observations and then using the fact that the model fits the observations to argue that the model is appropriate.

We are unsure which part of the manuscript you are referring to. If your comment is related to the transient simulations of ice-shelf growth in section 6, and the agreement between our modelled and observed reduction in surface speed after 10 years (Figure 4), then we believe this a genuine projection.

The initial model state is 'tuned' to reproduce the observed surface velocities for the given geometry by means of an optimal distribution of the rate factor, but ice shelf geometry, ice thickness and velocities are freely evolved after that. The advance of the ice front, enhanced ice-to-bed contact at the McDonald Ice Rumples and associated slow-down of the flow are non-trivial and obtained without further tuning.

5 A major caveat in our approach is the treatment of the rate factor, which was deliberately kept constant in our transient runs so we could assess the importance of a suitable 'damage model' or 'calving law' by comparing model output to observations. This rationale is now hopefully clear from section 6.

As noted earlier, there are different ways of representing rifts in a model and it is far from clear that the stress field associated with these different representations of rifts are equivalent. In fact, representing 10 rifts as discontinuities will generate stress concentrations near the tip of the rift that will not be present in models that represent rifts as diffuse zones of soft ice.

We hope to have addressed this point above, and refer to Appendix B, in particular figure B1, for more details.

Moreover, when tuning a model to match observations, it is often possible to absorb all uncertainties 15 and errors into the parameters that are being tuned. For example, in traditional damage mechanics, the damage affects the Cauchy stress and thus would also affect the driving stress on the right hand side of the SSA equations. Similarly, errors in density or briny layers of marine ice could also affect the driving stress. One can, of course absorb this error into inversions for the rate factor, but it is less clear that the inference of the rate factor is *physically* significant. Here, the authors can do more to make their case 20 by describing how rifts are represented in the model and showing actual maps of the rate factor and, if possible, converting those maps to physical variables, like equivalent ice temperature. Fortunately, the Brunt ice shelf itself appears to be well studied and the authors should be able to compare inversion results with the position of known bands of marine ice inferred by King et al.

We acknowledge the fact that the rate factor A, which has been tuned to minimize the misfit between 25 observed and modelled surface velocities, contains information about a variety of physical variables, including ice temperature and fractures. To demonstrate the physical significance of our results, we have provided several maps of A in Appendix A:

1) Figure A2, left panel: results for 1999, prior to rift formation. Away from shear margins and the fractured ice near the grounding line, we expect most of the variability to be related to the internal 30 structure of the ice shelf. Results do indeed distinguish between the bands of colder meteoric ice and surrounding areas of warmer marine ice, as identified by (Thomas 1973 and King et al., 2018).

2) Figure A2, right panel: results for 2016, after the activation of Chasm 1 and the Halloween Crack. Results are for a continuous mesh, and both rifts stand out as bands of weak ice, to accommodate the discontinuity in the flow field across the rifts. The contrast in stiffness (or temperature) between 35 meteoric ice and marine ice is also apparent here.

3) Figure B1, top row: results for 2016, but comparing results for a continuous mesh (left) to results from a mesh with holes (right). In both cases, the distribution of A is broadly similar, except for the absence of soft ice along the rifts in the case of a discontinuous mesh. Some small areas of soft ice remain, likely because the holes in the mesh were based on manual outlines of the rifts from visible 40 satellite imagery, and we were unable to capture the true extent of the active rifts using this method.

6

We get into similar issues when the authors argue that rift widening causes stress concentrations ahead of the rift. I don't follow the inference if all the authors have done is tune the model to match observations. The authors can, however, make this inference, if they have instead performed a forward model run and the widening of the rift predicted by the model matches observed widening rates and the stress increase near the tip of the rift matches the inferred stress increase. Again, this points to a need for some explanatory text.

Larour, E., et. al., (2014),Representation of sharp rifts and faults mechanics in modeling ice shelf flow dynamics: Application to Brunt/Stancomb-Wills Ice Shelf, Antarctica, J. Geophys. Res. Earth Surf., 119, 1918-1935, doi:10.1002/2014JF003157.

We did not perform any forward model simulations with evolving rift dynamics. Instead all stress maps are based upon a diagnostic analysis of an optimal model state (obtained through an inverse method) for successive velocity and geometry snapshots between 2000 and 2017. From these snapshots we infer significant changes in the stress distribution both before and after rift initiation, as discussed in sections 4 and 5.

3   Detailed comments

1. The introduction states that the focus of the manuscript is "on the more commonly neglected internal drivers that underlie rift initiation and propagation." It is far from clear to me that this accurately reflects the literature. For example, Fricker et al., 2002, Joughin and MacAyeal, 2005, Larour et al., 2004; Borstad et al., 2012 and 2017 all examine the glaciological stress as the dominant factor driving rift propagation. (There are many, many more citations. These are just a few examples. In fact, almost all of the literature that I can find points towards glaciological stress as the driver.)

We have provided further references to the literature in the introduction, and stressed the fact that all these studies suggest that stresses are an important driver for rift formation and propagation.

"Previous studies have suggested that glaciological stresses are a major control on rift formation and propagation, see e.g. Fricker et al., 2002, Joughin et al., 2005, Larour et al. 2004, Borstad et al., 2012, 2017, and the build-up of internal stresses within an ice shelf can generate energetically favourable conditions for the formation and propagation of rifts that cut through the full depth of the ice column (Rist, 2002). However, a direct link between changing stress conditions prior to calving, and the location and timing of rifts has not been demonstrated so far. This is in part due to the long characteristic time scales over which stresses evolve (typically multiple decades), and the lack of observational data required to calculate the stresses over the duration of a full calving cycle."

More recently (and in the Cryosphere) Arndt (2018) note the role of pinning points in generating rifts in Pine Island glacier, which seems analogous to the study here. In fact, as far as I can tell, with the exception of the Antarctic Peninsula Ice Shelves (that all seem to have effective social media accounts

and PR departments), most of the literature for ice shelves does focus on internal stresses. That said, the controls on rifting remain poorly understood, in part because of the long time scale between calving events make the process difficult to directly observe. This observational deficiency, in my opinion, is one of the more significant motivations and strengths of the present manuscript and it would be useful to re-emphasize this to readers.

We have expanded our motivation for this study in the introduction, and state that "The long-term observational record of the BIS provides unprecedented coverage of glaciological changes over a full calving cycle, from the last calving event in the early 1970s to present day.". We have stressed the importance of the McDonnald Ice Rumples (local pinning point) for the dynamics and its role as a trigger for calving. We have pointed out why lessons learnt for the Brunt Ice Shelf are lessons learnt for ice shelves elsewhere in Antarctica, and have referenced Arndt (2018) as an example. We will address this point in more detail in our reply to your next comment.

Fricker, HA, Young NW, Allison I, Coleman R. 2002. Iceberg calving from the Amery Ice Shelf, East Antarctica. Annals of Glaciology, Vol 34, 2002. 34

Joughin, I., and MacAyeal, D.R. (2005), Âa Calving of large tabular icebergs from iceˇ shelf rift systems, Âa Geophys. Res. Lett., 32, L02501, doi:10.1029/2004GL020978.ˇ

Larour, E., Rignot, E., and Aubry, D. (2004), Modelling of rift propagation on Ronne Ice Shelf, Antarctica, and sensitivity to climate change, Geophys. Res. Lett., 31, L16404, doi:10.1029/2004GL020077.

Borstad, C., McGrath, D., and Pope, A. (2017), Fracture propagation and stability of ice shelves governed by ice shelf heterogeneity, Geophys. Res. Lett., 44, 4186–4194, doi:10.1002/2017GL072648.

Borstad, C.P. et al. A damage mechanics assessment of the Larsen B ice shelf prior to collapse: Toward a physically-based calving law. Geophy. Res. Lett. 39, L18502 (2012).

Arndt, J. E., Larter, R. D., Friedl, P. , Gohl, K., Hoppner, K.Âaand ˇ athe Science Teamˇ of Expedition PS104, (2018): Bathymetric controls on calving processes at Pine Island Glacier , The Cryosphere, 12(6), pp. 2039–2050. doi:10.5194/tc-12-2039-2018

2. Iceberg calving is a natural process and this needs to be more clearly emphasized

The broader context in the introduction is the looming calving event from the Brunt Ice Shelf. Building on the previous point, it is known that ice shelves exhibit a natural cycle of decades to centuries advance punctuated by episodic retreat associated with the detachment of large tabular icebergs (see, Fricker et al., 2002, Walker et al., 2015). These calving events are believed to be driven by a combination of the accumulation of fractures coupled with changes in the glaciological stress. Yes, there is evidence for climate driven disintegration of ice shelves, primarily on the Antarctic Peninsula, but this is more of an exception to the norm. I suggest that the authors consider adding more context to the introduction, explaining not only that calving is part of the natural cycle of ice shelves, but how the calving event from the Brunt Ice Shelf fits into this larger context. How similar is this event from previous events? Or are are there no records of previous events? How does the cycle compare to other ice shelves?

The second paragraph of the introduction now starts with "Calving events are part of the natural life cycle of all ice shelves, as they go through internally-driven periods of growth and collapse (see e.g. Fricker et al., 2002, Anderson et al., 2014, Hogg et al., 2017)." and we have provided a broader context for the calving of the Brunt: "….As such, the cyclic dynamics of the BIS is modulated by natural changes in ice shelf geometry, and observations indicate that each cycle lasts approximately 40-50 years, which is comparable to other stable ice shelves (see e.g. Fricker et al., 2002).

The significance of local grounding at the MIR for the dynamics of the BIS, and its role in recent rifting events will be explored in subsequent chapters. However, the wider importance of pinning points for the dynamics and structural integrity of Antarctic ice shelves has been previously recognised (Borstad et al., 2013, Matsuoka et al., 2015, Favier et al., 2016, Berger et al., 2016, Gudmundsson et al., 2017), and their potential role in triggering calving events was highlighted recently for Pine Island Glacier (Arndt et al, 2018). Here we use the BIS as an example to demonstrate the link between naturally evolving glaciological conditions, the initiation of ice-shelf rifts, and the mechanical drivers that govern subsequent rift propagation. The geometrical configuration of the BIS is not unique, and similar principles likely apply to other Antarctic ice shelves that are dynamically constrained by local pinning points, such as the ice shelves in Dronning Maud Land (Favier et al., 2016) and the Larsen C Ice Shelf (Borstad et al., 2013). Our study is more generally relevant for ice shelves that experience a build-up of stress, potentially far upstream of the ice front, due to natural changes in ice-shelf geometry."

Similarly (and sorry for being pedantic), one of the issues that hindered my understanding of the broader context of the study is that the term "unique" is used frequently (4 times at least) and it was unclear what, exactly was unique in each of these instances?

The first time unique was used, it was used to describe the 50-year time series. This seems like appropriate usage. But, the next time we are told there is "a unique opportunity to enhance . . . process-based understanding". What is unique about the opportunity? Is this the 50-year time series? If this calving event is a continuation of the natural cycle, then (pedantically), the opportunity is not unique. There are also other rifts on other ice shelves that have been (or can be) studied. What exactly is unique about this opportunity/rift? The third time we are told there is a "unique, network of up to 15 GPS". GPS have been deployed around rifts (propagating and not propagating) in ice shelves multiple times so what about this particular deployment is unique. Finally, we are told "BIS represents a unique setting . . . . calving processes can be studied" This sounds like the authors are arguing that rift propagation/iceberg calving is different in this situation than the calving cycle that is observed elsewhere? It would be helpful to clarify all of this.

We understand your confusion and have either replaced "unique" by more appropriate wording, or removed it altogether. For example, we have replaced "Fortuitously, a **unique** opportunity to enhance our process-based understanding of rift dynamics and calving has recently arisen" by "Fortuitously, a **new** opportunity to enhance our process-based understanding of rift dynamics and calving has recently arisen"

Overall, I think that the authors could help readers understand the significant of the Brunt Ice Shelf and the particular rift system by sketching out what is common about the iceberg calving process across ice shelves. Then, tell us what is unusual in this situation (is it just the observations? the pinning point?) and what is truly unique here (is Brunt itself unique due to the large heterogeneities?). This would enable readers to better understand how this study fits into the broader context of rifting and calving from other ice shelves.

Walker, C., Bassis, J., Fricker, H., Czerwinski, R. (2015). Observations of interannual and spatial variability in rift propagation in the Amery Ice Shelf, Antarctica, 2002–14. Journal of Glaciology, 61(226), 243-252. doi:10.3189/2015JoG14J151.

We hope to have addressed this point in the introduction, as quoted above.

3. Methods, part 1 (inversions)

This is the where I really started to struggle to understand what was done and there is critical detail missing from the description of the model and inversion process. The model is described as a shallow-shelf approximation model SSA, which is standard for ice shelves. My understanding of the inversion is that the authors invert for the rate factor A(x,y) by ingesting surface velocities into the model. However, the inversion uses two regularization parameters γ_a and γ_s neither of which are defined in the text. Digging into Reese et al., 2018, it looks like the regularization parameters correspond to the ice softness AND basal friction coefficient. But an ice shelf, by definition, is freely floating and there is no basal friction. Are the authors inverting for basal friction beneath the pinning points? Is this done everywhere or in certain places? More details and more clarity are needed to understand what has been done here. I now see all the way at Page 8 that a Weertman sliding law is used specifically for the pinning points. This needs to be explained much earlier if it fits into the inversions. Also, what is the shape of the pinning point? Is the ice shelf plowing over it or is the pinning point just tickling the bottom?

We have rewritten this part of the methods and data section, and added a dedicated Appendix A with more details about the inverse method. The regularization parameters were defined, and results from an L-curve approach were added to motivate the chosen values. The description of the sliding law was moved to section 3, and additional details were added about the bedrock topography underneath the pinning point.

"Due to the inaccessibility and complex topography of the surface at the MIR, ground-based and airborne radar surveys have failed to reliably measure the bedrock topography in this location (Hodgson et al., 2019). In our analysis, the elevation of the bed was therefore set to 10m above the floatation depth across the extent of the MIR, and basal traction between the bed and ice was parameterized by a Weertman sliding law. The latter provides a commonly adopted relation between the basal sliding velocity vb and basal shear stress τb in grounded areas, $\tau_b = C^{(-1/m)} \|v_b\|^{(1/m-1)} v_b$, with m and C model parameters. A common value for the sliding exponent m = 3 was chosen, and the slipperiness coefficient was set to a spatially uniform value C = 10−3."

4.   Deviatoric stress is not constant with depth

There are also more subtle issues associated with the interpretation of the inferred rate factor. In the SSA approximation strain rate is independent of depth. However, the stress is only independent of depth if the temperature in the ice is constant within each column of ice. What the authors are really inferring is the depth averaged rate factor. A consequence is that the authors are also only able to show the depth averaged deviatoric stress. Stress could be much higher near the surface of the ice, where temperatures are likely much colder. This needs to be recognized and explained and in particular, related back to the physical interpretation of the rate factor of ice.

We acknowledge this fact and have made clear in the paper that *A* represents a vertically averaged value: "In general, *A* **varies spatially over several orders of magnitude (both horizontally and vertically),** and an alternative approach for estimating τ relies on commonly-used inverse theory, which uses observations of ice shelf geometry, velocity and ice thickness data to estimate an optimal spatial distribution of the rate factor *A(x)* by minimizing the mismatch between observed and simulated ice velocities (see e.g. MacAyeal, 1993 and Larour et al., 2005). The resulting solution for *A* and the diagnostic model output for $\dot{\epsilon}$ can be used to calculate a spatial distribution of the deviatoric stress τ and its principal components. **We used an adjoint iterative optimization method with Tikhonov regularization within the SSA (Shallow Shelf Approximation) ice flow model Úa (Gudmundsson et al, 2012) to obtain vertically-integrated values for** *A(x)* **and** $\tau(x)$**, where** *x* **denotes both horizontal dimensions**. Further details about the model setup, the inversion procedure and examples of *A(x)* for various ice-shelf configurations can be found in Appendix A."

5. Methods, part 2 (maps of rate factor please)

It helpful to readers to see the actual maps of inferred ice softness and basal friction (if this was also inverted for). This would certainly help convince readers that patterns of rate factor are realistic and not spurious artifacts. This is a matter of preference, but I personally also like to see the inferred rate factor converted into an ice temperature so that we can be sure that the ice temperature is semi-realistic based on known con ditions. The authors note that these are related to structural properties of the ice. In particular, it would be helpful to know if the inversions for ice softness correspond to regions of marine ice documented by King et al., (2018). In fact, one also wonders if the inversion could resolve the sharp variations in material properties associated with the bands of marine ice documented by King et al., (2018). A standard way to test this is by doing a "checkerboard" test. You compute the forward model using a checkerboard or other pattern. You then add noise to the signal and invert based on the synthetic data. This would give a sense of the resolution of the inversion and if the inversion can pick up relevant structural features. The more formal way of doing this would be to construct resolution kernels to formally determine what can and cannot be resolved.

We have provided maps of *A* and corresponding 'ice temperatures' for several ice-shelf configurations, both before and after rift initiation, in Appendix A. We comment on the physical meaning of these values, and discuss the broad spatial patterns, which indeed reflect previously identified variations in ice shelf structure (King et al., 2018).

6. Observations, how do you shift the data to a date?

I thought the observation section was much clearer and easier to understand. But it was unclear to me how you "shift" a DEM to an effective time step? There is no reference or description of the method used to do this. This, along with any error associated with the procedure should be described.

This has now been described in more detail in section 3:

"To correct for the ice motion between the different acquisition times of the WorldView-2 tiles, all tiles were translated to a common datum of 1 January 2013. For each tile, pixels were shifted by $\Delta x = u \Delta t$ with u(x) the surface velocity at location x obtained from a pair of Sentinel-1 images acquired in June 2015, and Δt the difference between the acquisition time of the tile and the common datum."

7. Can a viscous ice shelf model really accumulate stress at the tip of a rift by dissipating gravitational potential energy?

We did not include any prescription of dynamical rift evolution in our transient runs in section 6, but instead kept the rate factor constant and focussed on the discrepancies between observations and model output that resulted from the lack of an appropriate description of rift initiation and evolution. All maps of deviatoric stress in sections 4 and 5 are snapshots, based on an optimal estimate of the rate factor for given surface velocities and ice shelf geometry.

The authors argue that rift widening results in accumulation of stress ahead of the rift. The energy balance in an ice shelf model tells us that gravitational potential energy is dissipated through viscous flow. The accumulation of stress seems to imply energy is being added to the system faster than it can be removed. What is the source of the energy that is added to the system that drives energy accumulation? Is this related to torques associated with rotation of the blocks of ice? Is this conclusion supported by forward model runs or this based on tuning the model to match observations? Given the fact that rift widening is documented by GPS, it seems as though the authors should be able to do a forward model run to compare simulations with observed rift widening and use the forward model to show that stress is concentrated ahead of the rift.

Both Chasm 1 and the Halloween Crack have been observed to widen at slowly accelerating rates for weeks to months, without noticeable propagation (De Rydt et al., 2018). The widening of both rifts results from the rotational motion of the soon-to-be-icebergs away from the main ice shelf, and the resulting torque is either dissipated through viscous deformation or stored until further rift propagation occurs. We did not estimate the energy balance or perform a forward simulation with a description of the rift dynamics, which would generally require a viscoelastic treatment with fracture propagation criteria such as VCCT or the J-integral. Instead our (much less ambitious) aim was to detect changes in the far-field stress distribution of the ice shelf through snapshot inversions of surface velocity and ice shelf geometry using an SSA model, and diagnose the optimal model state for its stress configuration at various times. The results are presented in sections 4 and 5.

8. Conclusions
This is up to the author, but there has been little doubt that "calving laws" are needed in ice sheet models and this is not the main conclusion I would draw from this study. I don't think it will come as any surprise to most readers that iceberg calving is an important process in ice sheet evolution. The authors also have a typo in their description of the so-called marine ice cliff instability. The marine ice

cliff instability assumes that there is a **maximum** ice thickness, not a **minimum** ice thickness. Moreover, the marine ice cliff instability generally applies to thick grounded ice and not thin ice shelves, like the Brunt Ice Shelf. Minimum ice thickness models have been a mainstay in ice sheet models for decades largely as a means of preventing ice shelves from indefinitely advancing. Hence, the authors have a good argument that these minimum thickness criteria are not physical.

Actually, coming back to the Deconto and Pollard marine ice cliff instability study, my understanding is that the parameters used by Deconto and Pollard were derived based on parameter sensitivity studies for past sea level rise. These are, technically, observations are they not? Direct observations of ice flow of ice sheets hundreds of thousands of years ago, similar to the GPS and satellite imagery used in this study, remains a challenging problem in paleo ice sheet studies. And if the marine ice cliff instability is really a thing, the only evidence we have likely comes from past ice sheet conditions when these processes may have been active. Here, it would be useful if the authors put their results in context of past and future projections of ice sheet change. If structural heterogeneity is important, is it possible to predict it instead of tuning a model to match observations? How important is structural heterogeneity versus the geometry of pinning points? It seems like knowing the location of pinning points (which is possible) could at least provide a first order approach to rift generation even if it does not match the detailed sub-decadal trends? This study potentially offers a lot of information and it would be useful to readers to see how this fits into the bigger picture.

We think these are all very valid points and have reformulated the conclusions to better reflect these thoughts:
"Our results, based on observations and numerical modelling, demonstrate how ice shelves that are dynamically constrained by local pinning points, such as the Brunt Ice Shelf, can experience significant changes in internal stress caused by their naturally evolving geometry, and generate favourable conditions for rifting far upstream of the ice front. Such conditions make these ice shelves particularly susceptible to fast collapse, a process that is not generally captured by present-day ice flow models, despite recent progress (Levermann et al., 2012; Borstad et al., 2012). Existing calving criteria based on a maximum ice thickness, such as the marine ice-cliff instability mechanism (De Conto and Pollard, 2016), remain controversial and might not be directly relevant for thin floating areas such as the BIS. Other commonly-used calving laws based on minimum ice thickness criteria discard variations in mechanical properties of the ice, and are independent of internal stress. Existing theories for the vertical propagation of surface and basal crevasses (Hughes, 1983, van der Veen, 1998a, 1998b), often linked to surface hydrology (Scambos et al, 2000, Scambos et al., 2009, Nick et al., 2013), do not generally include criteria for the initiation and horizontal propagation of full-depth rifts. As a result, model simulations do not generally capture rapid and large-scale changes in ice shelf geometry, and thereby underestimate the critical role of ice shelves as a buffer against further mass loss from the Antarctic Ice Sheet."

Minor comments:

Page 5, line 25: What is "Geometric Deformation"? Do the authors mean that the geometry of the ice shelf is changing? I actually googled this term, but all of the hits directed me to papers on differential geometry, which seems like it is not what the authors are talking about.

Changed to "changes in the ice shelf's geometry"

5

Page 6, line 26. Ice is in hydrostatic equilibrium. A force balance at the ice-ocean interface (analogous to that at the calving front) within a melange free rift suggests a deviatoric stress pointing into the rift. Why is the ocean pressure pulling the rift apart? The large scale stress of the ice shelf might pull the ice apart. This should be clarified.

10   We have replaced this line by a more precise statement "Following rift propagation, newly formed rift surfaces were subjected to ocean pressure, and stresses within the ice shelf gradually adjusted to the new boundary conditions and newly emerging ice front location. In particular, maximum tensile stresses aligned perpendicular to the edges of the rifts."

15   Page 3, line 28: We were told there is 50 years of data, why only focus on the period from 1997-2018? What is the benefit of the long time series if less than half are used? The earlier emphasis on 50 years of data seems like a bit misleading at this point.

Different parts of the long-term record have been used for different purposes. The 1915-1970s data have provided valuable context for present-day events because it has allowed us to describe the ongoing
20   calving as 'reoccurring'. The 1999-2017 data with full spatial coverage of the ice shelf, on the other hand, has allowed us to analyse ice-shelf wide changes in the flow and stresses before and after rift initiation. We have changed the abstract to " …20-years' time series of in-situ and remote sensing observations.." but have put emphasis on the use of the long-term record at various places in the introduction.

25   Page 1, line 20: This is pedantic, but I would consider the 5000 km^2 berg that detached from the Larsen Ice Shelf to be a small to mid-sized berg. Iceberg B15 that detached from the Ross Ice Shelf was twice as large and Shackleton documented icebergs that were even larger.

We meant 'large' compared to the size of calving events caused by bending stresses near the ice front.

Page 1, line 20: The word "since" refers to time. For example, "It has been a long time since the Knicks
30   won the championship." In this case, I believe you want "Because".

Corrected.

Page 2, line 9: The references given here document thinning of ice shelves and do not appear to describe any links between thinning and calving.

This paragraph has been removed.

35   Everywhere: space between numbers and units 3m should be 3 m

Corrected.

Page 7, line 2: comma after "but"

Corrected.

Page 7, 2nd paragraph: Now I'm really confused about what is going on. Are the authors introducing a rift into the model and widening it, based on observations to examine the stress field. Or, have the authors inverted for stress (OK, actually ice softness) based on surface velocities at several intervals of time? In the first case, I think the authors are safe saying that the increase in stress is due to rift widening. In the second case, I don't know that you can say that the stress is caused by widening when no rift widening has been included in the model and the model has been tuned to reproduce surface velocities (and hence stresses). Morever, the assumption that rift widening results in stress concentration should be checked against other periods of time when rift propagation did not occur. For example, there is a long history of rift widening without propagating prior to Chasm's reactivation. Does this period of time correspond to the rift propagating into a zone of marine ice?

We follow the second approach, i.e. invert for stresses to match different snapshots of surface velocity and ice shelf geometry (incl. rift extent, ice front location and surface elevation). Based on this method, significant changes in stress are found between successive time stamps. These are interpreted as the combined effect of changes in local grounding at the MIR, changes in rift extent and width, and overall deformation of the ice. We agree that they cannot be attributed to rift widening alone, and we have removed this statement from the paper.

Page 7, line 26: The technical jargon "damage" is introduced here. Authors should avoid the term or define it. Keep in mind that "damage" has a precise definition in the fracture mechanics literature and is, most generally, a tensor. The term damage is often used heuristically in glaciology in confusing and imprecise ways. If the authors mean rifting, I recommend just saying rifting.

We have replaced the term "damage" by "rift" or "fracture" throughout the manuscript.

Section 6, Page 8, section paragraph: Wait a minute. Why is the rate factor A(x,y) not a property of ice that advects with the ice? Conventionally, the rate factor has been linked to temperature, grain size and crystal structure of the ice. If reductions in the factor A(x,y) are linked to fractures then surely these must also advect with the ice? If the advection of the rate factor is not important, then why is heterogeneity of the ice important? I'm missing something critical here because this seems like this contradicts the authors main conclusion that heterogeneity is important.

Rather than simulating changes in *A* to reflect fractures and aiming to reproduce observations as closely as possible, in section 6 we analysed discrepancies between observations and transient model output for a constant rate factor. As we pointed out in the paper, projections with constant *A* over century to millennium timescales are still common practice, and this approximation might not be justified in certain cases. Our experiment in section 6 led to two main results: 1) between 2000 and 2010 (i.e. before rift initiation) the model is capable of reproducing the observed slow-down of the Brunt Ice Shelf as a result of increased buttressing at the pinning point. In other words, the SSA model does an ok job at reproducing the conditions that eventually caused fracture formation, even with a constant rate factor. 2) After 2012 and the initiation of Chasm 1 and the Halloween Crack, model projections with a constant rate factor started to deviate significantly from observations (up to 100%). This was expected, and

almost entirely due to the lack of a suitable description of fracture initiation and propagation. Our approach has allowed us to quantify errors related to the lack of an appropriate treatment of fractures (by means of changes to *A* or other), and has demonstrated the need for such a treatment for certain ice shelves, even at decadal timescales.

5   The "extrusion" method for calving front advance is known to generate significant artifacts if not treated carefully. The calving front should advect as a sharp shock and accurate shock capturing methods are needed to avoid overly diffusing the calving front. Numerical details of advection should be included with limitations described. Does the advection scheme preserve mass? It is diffusive? Does it preserve the shock-like nature of the calving front? Are results sensitive to grid size or time step size?

10

In the Figure below we show sections of the transient ice shelf geometry for two flowlines: at the top is a flowline towards the east of the pinning point (Gaussian bump in the figure), and at the bottom is a flowline through the middle of the pinning point. Different colours indicate different years, with blue curves corresponding to the (ungrounded) 2000 geometry, and red the 2010 geometry after re-

15   grounding onto the pinning point. As can be seen from the top panel, the ice front remains relatively well-defined when not distorted by the bedrock, as is the case in the lower panel. As pointed out in the paper, "A fully implicit time integration with streamline upwind Petrov-Galerkin method and stabilization (SUPG) was used, and the ice front was found to advance with limited diffusion or spurious oscillations."

20

Flowline geometries
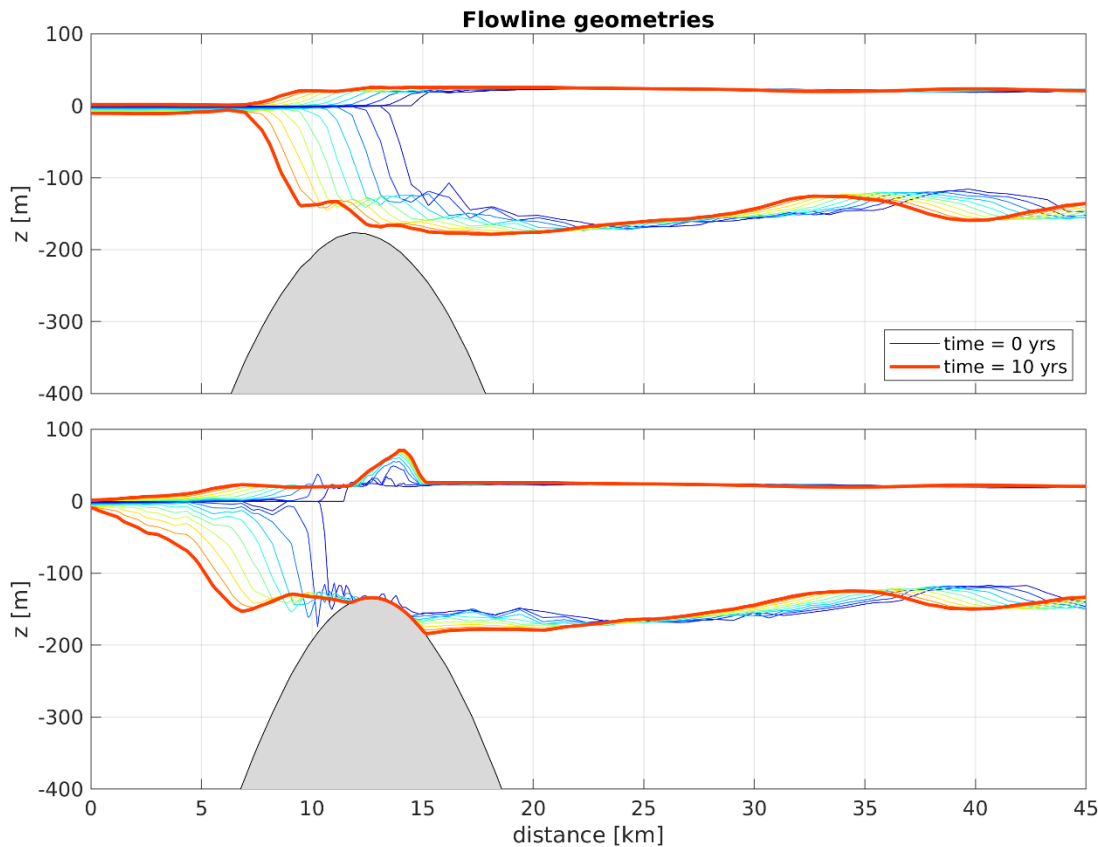
Page 8, last paragraph: The statement that ice sheet models keep the calving front pinned to present day conditions might have been true a decade or two ago, but pretty much all of the major ice sheet models at this point allow the calving front to evolve. PISM uses a wetting drying algorithm combined with "eigen calving". ISSM uses a level set method combined with a Von Mises calving law. BISICLES and CISM have their own methods to advance the calving front and use a spectrum of calving laws. These days, models allow the calving front to advance and retreat according to heuristic (and often known to be incorrect) parameterizations. Whether advancing and retreating the calving front based on inaccurate and unphysical calving laws is progress is a question that I will leave to others.

We agree that several models have at least some capability to advance or retreat their ice fronts. We have removed this statement from the text.

Page 12, line 12: Reference to Lipovsky, 2018b appears to reference an unpublished manuscript. Check Cryosphere style guidelines for rules on references to non-peer reviewed literature. This is prohibited by AGU publications, but the standards of TCD might not be as stringent

Reference has been removed.

Figure 2-3. Best not to use a red-green color scale.

This color scale was tested by and deemed suitable for colorblind people, unless there are other reasons not to use a red-green color scale?

5

Calving cycle of the Brunt Ice Shelf, Antarctica, driven by changes in ice-shelf geometry

Jan De Rydt[1], G. Hilmar Gudmundsson[1], Thomas Nagler[2], Jan Wuite[2]

[1]Department of Geography and Environmental Sciences, Northumbria University, Newcastle upon Tyne, UK.
[2]ENVEO – Environmental Earth Observation, Innsbruck, Austria.

Correspondence to: Jan De Rydt (jan.rydt@northumbria.ac.uk)

Abstract. Despite the potentially detrimental impact of large-scale calving events on the geometry and ice flow of the Antarctic Ice Sheet, little is known about the processes that drive rift formation prior to calving, or what controls the timing of these events. The Brunt Ice Shelf in East Antarctica presents a rare natural laboratory to study these processes, following the recent formation of two rifts, each now exceeding 50 km in length. Here we use two decades of in-situ and remote sensing observations, together with numerical modelling, to reveal how slow changes in ice shelf geometry over time caused build-up of mechanical tension far upstream of the ice front, and culminated in rift formation and a significant speed-up of the ice shelf. These internal feedbacks, whereby ice shelves generate the very conditions that lead to their own (partial) disintegration, are currently missing from ice flow models, which severely limits their ability to accurately predict future sea level rise.

1 Introduction

Icebergs that calve from the floating margins of the Antarctic Ice Sheet account for up to 50% of ice discharge into the Southern Ocean (Depoorter et al., 2013). The largest calving events, such as the loss of a 5000 km^2 iceberg from the Larsen C Ice Shelf in 2017 (Hogg and Gudmundsson, 2017), result from the horizontal lengthening of multi-kilometre long rifts that cut through the full thickness of the ice. These large-scale events, in contrast to the loss of small ice blocks in the bending zone near the ice front (Reeh, 1968), significantly reshape the geometry of the ice-shelf margins, and can have a profound impact on their structural integrity (Doake et al., 1998). Because ice shelves act as a barrier around the grounded ice and buttress its seaward flow through lateral drag and local grounding in shallow water (Dupont and Alley, 2005), any loss of buttressing around the periphery of Antarctica as a result of calving-induced changes in ice-shelf geometry will adversely affect glacier flow (Scambos et al., 2004, Rignot et al., 2004, Rott et al., 2011), and induce additional ice discharge into the Southern Ocean.

Larger calving events are part of the natural life cycle of all ice shelves, as they go through internally-driven periods of growth and collapse (see e.g. Fricker et al., 2002, Anderson et al., 2014, Hogg et al., 2017). Despite the importance of calving for the mass balance of the Antarctic Ice Sheet, detailed observations of such events and related changes in ice-shelf dynamics remain

scarce. In particular, conditions for full-depth fracture and the subsequent propagation of kilometre-scale rifts are poorly understood. Previous studies have suggested that glaciological stresses are a major control on rift formation and propagation, see e.g. Fricker et al., 2002, Joughin et al., 2005, Larour et al. 2004, Borstad et al., 2012, 2017, and the build-up of internal stresses within an ice shelf generate energetically favourable conditions for the formation and propagation of rifts that cut

5   through the full depth of the ice column (Rist, 2002). However, a direct link between changing stress conditions prior to calving, and the location and timing of rifts has not been demonstrated so far. This is in part due to the long characteristic time scales over which stresses evolve (typically multiple decades), and the lack of observational data required to calculate the stresses over the duration of a full calving cycle.

10   Once initiated, ice shelf rifts have been shown to lengthen at rates that vary strongly in time (Bassis et al., 2005, Walker et al., 2015, Borstad et al., 2017, De Rydt et al., 2018), from meters to kilometres per day, and can arrest for extended periods. Suture zones of basally accreted marine ice have been linked to periods of slow rift propagation and could delay or halt large-scale calving (Borstad et al., 2017). Contrasting observations have reported fast unzipping of rifts along bands of marine ice and slow propagation through meteoric ice (De Rydt et al., 2018, King et al., 2018), highlighting the complex nature of rift

15   behaviour. At present, a unified formulation of rift dynamics rooted in existing theory of fracture mechanics is still under development (Rist et al., 2002, Bassis et al., 2008, Lipovsky, 2018). As a result, predictions for the location and timing of large-scale calving events remain ill-constrained and the feedback between calving rates and ongoing climate-change induced thinning of ice shelves (Pritchard et al., 2009, Flament and Remy, 2012, Konrad et al., 2016) or changes in the internal structure of the ice are unknown.

20

Fortuitously, a new opportunity to enhance our process-based understanding of rift dynamics and calving has recently arisen with the impending calving of two tabular icebergs from the Brunt Ice Shelf (BIS) in East Antarctica (Figure 1a). In December 2012 a historical rift structure, 'Chasm 1', that had lain dormant for three decades (Figure 1b), was reactivated and started to lengthen by several kilometres per year (De Rydt et al., 2018). The renewed rifting activity was followed by the formation of

25   a second rift, the so-called 'Halloween Crack' in October 2016 (De Rydt et al., 2018), which grew quickly and reached a length of 60 km by October 2018 (Figure 1b). Both Chasm 1 and the Halloween Crack continue to grow to date.

Changes in dynamics of the BIS have been documented in great detail before and after rift formation, and the behaviour of both rifts has been monitored closely since the day of their initiation, in part by an extensive network of up to 15 permanent

30   GPS stations (Gudmundsson et al., 2017, De Rydt et al., 2018). Furthermore, recent advances in satellite data availability have provided a comprehensive spatial and temporal description of the flow and ice deformation across the ice shelf (Thomas, 1973, Simmons and Rouse, 1984, Simmons, 1986, Gudmundsson et al., 2017). In addition, the continuous occupation of the Halley Research Station on the ice shelf since the mid-1950s and a long-term glaciological monitoring programme, has allowed us to put ongoing changes into a historical perspective.

The long-term observational record of the BIS provides unprecedented coverage of glaciological changes over a full calving cycle, from the last calving event in the early 1970s to present day. Based on this record and earlier observations of the ice front location in 1915, 1958 and 1986 (Anderson et al., 2014) and flow speed measurements since the 1950s (Gudmundsson et al, 2017), a cyclic pattern of glaciological changes emerges. First, calving and ice front retreat caused a loss of pinning from a small seabed shoal (McDonald Ice Rumples or MIR in Figure 1a), which triggered an acceleration of the flow. Subsequently, expansion of the ice shelf and local regrounding at the MIR lead to a slow increase in buttressing and deceleration of the flow. As such, the cyclic dynamics of the BIS is modulated by natural changes in ice shelf geometry, and observations indicate that each cycle lasts approximately 40-50 years, which is comparable to other stable ice shelves (see e.g. Fricker et al., 2002).

The significance of local grounding at the MIR for the dynamics of the BIS, and its role in recent rifting events will be explored in subsequent chapters. However, the wider importance of pinning points for the dynamics and structural integrity of Antarctic ice shelves has been previously recognised (Borstad et al., 2013, Matsuoka et al., 2015, Favier et al., 2016, Berger et al., 2016, Gudmundsson et al., 2017), and their potential role in triggering calving events was highlighted recently for Pine Island Glacier (Arndt et al, 2018). Here we use the BIS as an example to demonstrate the link between naturally evolving glaciological conditions, the initiation of ice-shelf rifts, and the mechanical drivers that govern subsequent rift propagation. The geometrical configuration of the BIS is not unique, and similar principles likely apply to other Antarctic ice shelves that are dynamically constrained by local pinning points, such as the ice shelves in Dronning Maud Land (Favier et al., 2016) and the Larsen C Ice Shelf (Borstad et al., 2013). Our study is more generally relevant for ice shelves that experience a build-up of stress, potentially far upstream of the ice front, due to natural changes in ice-shelf geometry.

The paper is organized as follows. In section 2 we provide a brief overview of the historical and ongoing glaciological changes on the BIS, and argue how these changes are part of the natural lifecycle of the ice shelf. In section 3 we introduce the tools and data that were used to diagnose the glaciological conditions that gave rise to the initiation and propagation of Chasm 1 and the Halloween Crack. The results are divided into 3 parts: in section 4 we present a timeline of changes in glaciological stress that led to the initiation of the rifts; in section 5 we discuss the drivers of subsequent rift propagation; in section 6 we compare the observed dynamical changes before and after rift formation to model projections, and quantify model errors related to the absence of a suitable calving law. Conclusions are presented in section 7.

2 Historical context and the calving cycle of the Brunt Ice Shelf

In the early 1970s, a single calving event significantly reduced the extent of the BIS (Thomas, 1973), and the retreat of the ice front caused a loss of contact between the ice base and a seabed shoal at the McDonald Ice Rumples (MIR, Figure 1a). The localized loss of friction with the seabed resulted in a reduction of the backstress (or buttressing) and coincided with a twofold

increase in flow speed of the remainder of the ice shelf (Simmons and Rouse, 1984, Gudmundsson et al., 2017). This speed-up unequivocally demonstrated the potential impact of geometrical changes on ice-shelf dynamics. In decades following, the ice front re-advanced by up to 30 km in places (Figure 1b) and the deforming ice gradually re-established ice-to-bed contact at the MIR, causing the ice shelf to slow down to pre-calving speeds by 2012 (Gudmundsson et al., 2017).

5

The dramatic succession of speed-up and slow-down by over 100% within a few decades comprises some of the highest amplitude variations in flow speed observed in Antarctica, and we argue that these changes are driven entirely by internal ice dynamics processes. The BIS, which is situated on the eastern edge of the Weddell Sea, has not been affected noticeably by changes in external conditions during recent decades. Sustained negative surface temperatures throughout the year prevent

10 surface melting (Anderson et al., 2014) and eliminate the risk of crevasse penetration caused by hydrofracturing (Scambos et al., 2000) and potential weakening of the ice shelf. There is also no indication that offshore Modified Warm Deep Water intrudes into the ice shelf cavity to cause significant basal ablation (Nicholls et al., 2009) or ice-shelf thinning (Paolo et al, 2015). As a result, the BIS represents a unique setting in which large-scale calving processes can be studied in relative isolation, and the wealth of available data can be probed to gain unbiased insights into the mechanics of ice-shelf fracture.

15

In 2012, following four decades of ice shelf growth, the ice front of the BIS reached its most advanced position since the beginning of measurements in 1915 (Anderson et al., 2014). The advance of the ice front coincided with local grounding of the ice shelf at the MIR over a small but prominent area of 5 km^2. At the same time, preconditions for rifting were re-established (as will be explained in section 4), and the reactivation of Chasm 1 in December 2012 and formation of the Halloween Crack

20 in October 2016 marked the start of two new calving events. Their combined impact is expected to reduce the ice shelf's area by more than 50% (De Rydt et al., 2018), the largest single perturbation in ice shelf geometry on record. In response to the damage caused, a renewed increase in flow speed by up to 10% per year was observed between 2012 and present-day across most of the ice shelf (Figure 1b and (Gudmundsson et al., 2017)).

25 Based on this 50-year record of ice geometry and flow speed, the BIS appears to exhibit successive phases of fast acceleration and slow deceleration of the flow, modulated by changes in geometry and buttressing at the MIR. In subsequent sections we investigate how these changes in glacio-mechanical conditions led to the reactivation of Chasm 1 in 2012 and caused the initiation of the Halloween Crack in October 2016 at the observed location.

3 Methods and data

30 In order to investigate the timing and location of rifting in relation to mechanical changes in the ice shelf, we use spatial maps of principal stress magnitude and direction as a diagnostic tool. The maximum principal stress magnitude is used in fracture mechanics as a criterion to identify when brittle materials fail under tension, see e.g. Rist et al., 2002. Although we do not aim

to formulate the details of such a fracture criterion here, or discuss complications due to the brittle-ductile properties of ice, we acknowledge the potential effect of high stress concentrations (or load) on the structural integrity of the ice. We analyse maximum principal stress patterns for 9 different configurations of the BIS between 1997 and 2018, based on snapshot observations of surface velocity, ice thickness and ice shelf extent (Table 1). We subsequently relate spatiotemporal changes

5   in the principal stress to the observed timing and location of rifting events.

3.1 Calculation of horizontal stresses

The elements of the stress tensor cannot be measured directly, but are related to the strain rates $\dot{\epsilon}$ and rate factor A through the material rheology, described by Glen's Law:

(1) $\dot{\epsilon} = A\tau_E^{n-1}\tau,$

10   with τ the deviatoric stress tensor and $n=3$ the creep exponent. In ice bodies with a uniform rate factor A, horizontal strain rates can be calculated directly from observed surface velocities, and Eq. (1) implies an estimate for the deviatoric stresses and the associated principal components.

In general, A varies spatially over several orders of magnitude (both horizontally and vertically), and an alternative approach
15   for estimating τ relies on commonly-used inverse theory, which uses observations of ice shelf geometry, velocity and ice thickness data to estimate an optimal spatial distribution of the rate factor $A(\vec{x})$ by minimizing the mismatch between observed and simulated ice velocities (see e.g. MacAyeal, 1993 and Larour et al., 2005). The resulting solution for A and the diagnostic model output for $\dot{\epsilon}$ can be used to calculate a spatial distribution of the deviatoric stress τ and its principal components. We used an adjoint iterative optimization method with Tikhonov regularization within the SSA (Shallow Shelf Approximation)
20   ice flow model Úa (Gudmundsson et al, 2012) to obtain vertically-integrated values for $A(\vec{x})$ and $\tau(\vec{x})$, where $\vec{x}$ denotes both horizontal dimensions. Further details about the model setup, the inversion procedure and examples of $A(\vec{x})$ for various ice-shelf configurations can be found in Appendix A.

3.2 Observational datasets

The inverse method requires input from three key observational datasets: ice thickness, surface velocity and ice-shelf extent
25   (i.e., ice front and grounding line location). In this study, inversions for 9 successive ice shelf configurations between 1997 and 2018 were carried out, giving 9 snapshots of the horizontal stress distribution in the ice shelf. More details about the data sources for each of these configurations can be found in Table 1. Additional data from intermediate times, in particular MEaSUREs and Sentinel-1 velocity fields, are available and can be used to obtain a denser time series of stress patterns. However, analysis of the additional data did not contain any new findings beyond those presented.

30

23

Ice thickness estimates were derived from a digital elevation model (DEM) and a flotation criterion assuming a two-layer density model with a 30 m firn layer (ρ_{firn}= 750 kg/m^3) overlaying solid ice (ρ_{ice}= 920 kg/m^3) (De Rydt et al., 2018). For the 01/01/1999 stress calculation, the Bedmap 2 surface DEM was used. For all other stress calculations, a new DEM was generated from a mosaic of 3m horizontal resolution WorldView-2 tiles acquired between 19 October 2012 and 30 March 2014 (covering the Brunt Ice Shelf) and Cryosat-2 data (Slater et al., 2018) (covering the Stancomb-Wills Glacier Tongue). To correct for the ice motion between the different acquisition times of the WorldView-2 tiles, all tiles were translated to a common datum of 1 January 2013. For each tile, pixels were shifted by $\Delta\vec{x} = \vec{u}\,\Delta t$ with $\vec{u}(\vec{x})$ the surface velocity at location $\vec{x}$ obtained from a pair of Sentinel-1 images acquired in June 2015, and Δt the difference between the acquisition time of the tile and the common datum. Subsequently, a constant vertical shift was applied to each tile to minimize the misfit in overlapping regions. The resulting surface DEM was compared to 5000 km of in situ airborne Light Detection And Ranging (LiDAR) data acquired in January 2017 (Hodgson et al., 2019) and referenced with respect to sea level using 8 LiDAR sections over the open ocean. The mean difference between the resulting DEM and LiDAR data in overlapping regions was 0.01±3.6 m.

Surface velocity data were acquired from a variety of sources, as detailed in column 3 in Table 1. Velocity fields based on Sentinel-1 data were processed using an iterative offset tracking method (Nagler et al., 2015). To account for tidal artefacts, all velocity maps were cross-calibrated to high-precision GPS data from a long-term network of up to 15 dual frequency GPS receivers on the BIS (Anderson et al., 2014, Gudmundsson et al., 2017, De Rydt et al., 2018 and Figure 1a). The GPS data were processed using PPP techniques using the Bernese software to obtain daily positions with sub-centimetre precision. For each horizontal velocity component, a linear regression between satellite data and GPS displacements over the corresponding satellite acquisition period was used to calculate the mean offset between both datasets. The offset was subtracted from satellite-derived estimates of surface velocity in order to ensure an optimal fit between the latter and in situ GPS data. Each final velocity product was assigned an effective timestamp corresponding to the middle of the feature tracking window (first column in Table 1). In order to guarantee consistency between the surface velocity and DEM in the model inversion, the DEM was translated to the velocity timestamp using the method described above.

Ice front positions were outlined from Landsat-7/8 cloud-free panchromatic band images (column 4 in Table 1). The temporally varying extent of grounding at the MIR was derived from a combination of proxy indicators, in particular crevasse patterns, surface velocity data and surface elevation. Due to the inaccessibility and complex topography of the surface at the MIR, ground-based and airborne radar surveys have failed to reliably measure the bedrock topography in this location (Hodgson et al., 2019). In our analysis, the elevation of the bed was therefore set to 10m above the floatation depth across the extent of the MIR, and basal traction between the bed and ice was parameterized by a Weertman sliding law. The latter provides a commonly adopted relation between the basal sliding velocity v_b and basal shear stress τ_b in grounded areas, $\tau_b = C^{-1/m}\|v_b\|^{\frac{1}{m}-1}v_b$, with

m and *C* model parameters. A common value for the sliding exponent *m* = 3 was chosen, and the slipperiness coefficient was set to a spatially uniform value $C = 10^{-3}$.

4 Ice-shelf growth causes rifting

Figure 2 shows a time series of the principal stress directions (arrows) and maximal principal deviatoric stress (colours) in the
5   horizontal plane, covering 12 years before to 4 years after the reactivation of Chasm 1 in December 2012. Before 2000 (Figure 2a), the stress pattern is characteristic for a nearly free floating (or unbuttressed) ice shelf, with most areas showing extensive deviatoric stresses in both principal directions. Note that at this time, grounding at the MIR was restricted to a small area of about 1 km^2, which caused higher-than-average stresses at the ice front in this area (Figure 2a), but limited upstream buttressing. Between 2000 and 2007 (Figure 2b), a fast and sharp transition occurred from a purely tensile to a mixed
10   tensile/compressive regime, with compressive stress trajectories radially aligned around the MIR. This pattern is characteristic of a point pressure source located at the MIR, and supports the notion that growing contact between the ice base and sea floor caused an increase in backpressure in this area. With the onset of compression, tensile stresses increased by more than twofold, with the largest values found 10 km upstream of the MIR. Between 2007 and 2013 (Figure 2c), the zone of high tension expanded and spread outward from the MIR, with values up to 120 kPa. Once the periphery of this zone reached the historical
15   rift tip of Chasm 1 in December 2012, the ice shelf eventually fractured along this line of pre-existing weakness (Figure 2c).

After the initiation and sub-critical propagation of Chasm 1 in December 2012, stress values on the western shelf significantly reduced between 2013 and 2016. Simultaneously, bands of high tension developed towards the east of the MIR (Figure 2d) with estimated tensile deviatoric stress values up to 140 kPa. These bands show no obvious spatial correlation to variations in
20   ice thickness or internal ice structure (King et al., 2018). On 4 October 2016, the ice shelf fractured within the band nearest and about 15 km upstream of the MIR (Figure 2d). Following rift initiation, the Halloween Crack rapidly propagated towards the MIR and in the opposing eastward direction along trajectories perpendicular to the local maximal tensile stress direction (Figure 3b and e).

25   Our calculations provide a simple and intuitive explanation for the sudden reactivation of Chasm 1 in December 2012 and the formation of the Halloween Crack in October 2016. The timing of both rift initiations, the location and the subsequent propagation paths can all be explained in relation to the magnitude and orientation of the tensile deviatoric stress distribution (Figure 2). In both cases, the rifts formed in response to a gradual build-up of horizontal tensile stresses that took place over decades as the ice shelf expanded over time, and increased its contact with the seabed at the MIR. The locations of initiation
30   were consistent with the hypothesis that ice-shelf areas subjected to the highest tensile stress are most susceptible to failure. A priori, these favourable conditions, dictated by changes in geometry, are not restricted to areas close to the ice front or within the shear margins. In particular, they can occur landward of the compressive arch, which is the transition zone between freely

floating (or passive) ice close to the ice front, and upstream ice in compression (Doake et al., 1998, Fürst et al., 2016). Rifts that cut through the compressive arch, as is the case for the Halloween Crack, will affect the buttressing capacity of the ice shelf, and thereby induce changes in ice shelf dynamics or continue to affect its structural integrity (Doake et al., 1998).

5 Discontinuous rift propagation

5 Following the initiation of both rifts, the sustained deformation of the ice shelf's geometry and reduction in load-bearing capacity due to rift propagation, caused progressive changes in the large-scale stress pattern. As previously noted, the formation of Chasm 1 coincided with an increase in deviatoric stress towards the south and east of the MIR, which likely contributed to the formation of the Halloween Crack (Figures 2c-d). Following rift propagation, newly formed rift surfaces were subjected to ocean pressure, and forces within the ice shelf adjusted to the new boundary conditions and newly emerging ice front

10 location. In particular, maximum tensile stresses aligned perpendicular to the edges of the rifts.

In Figure 3, principal stress patterns for 5 different ice shelf geometries between December 2016 and October 2017 are shown, demonstrating the changes as Chasm 1 and the Halloween Crack propagated. In November 2016, the tip of the Halloween Crack stagnated within a prominent zone of high tensile stress (Figure 3a) for a 4-week period, despite persistent rift widening

15 (De Rydt et al., 2018). It was previously noted that this area consists of a complex conglomerate of thick meteoric ice and thinner marine ice (De Rydt et al., 2018, King et al., 2018), and such inhomogeneities have the potential to slow down rift propagation. From around 15 December 2016, the period of slow changes in rift length and high concentrations of remotely-applied stress was followed by a period of fast propagation as the rift cut through an area of relatively homogeneous marine ice. By 29 December 2016, the Halloween Crack had propagated a further 11 kilometres at an average rate of 800 m/day

20 (compared to <100 m/day in November). Following this event, a significant reduction in the calculated tensile stress (Figure 3b) indicated an efficient release of stress through fracture propagation.

Similar changes in the far-field stress were observed between January 2017 and October 2017 in the vicinity of Chasm 1. Preceding this period, the location of the rift tip remained relatively stationary for about 12 months in a transition zone between

25 thin (~ 100 m) marine ice and a band of regularly spaced blocks of thicker (~ 150-200 m) meteoric ice (King et al., 2018). Yet, GPS stations located on both sides of the rift indicated a slowly accelerating increase in its aperture (De Rydt et al., 2018) due to the rotation of the ice downstream of Chasm 1 towards the west and away from the remaining shelf (see Figure 1b). The period of increasing torque and slow lengthening coincided with a build-up of tensile deviatoric stress within the band of meteoric ice ahead of the rift tip (Figure 3c and d) with values estimated up to 120 kPa. In 2017, a phase of rapid propagation

30 followed, the onset of which was detected in January 2017 (De Rydt et al., 2018). By late October 2017, Chasm 1 had lengthened by about 4.5 km (Figure 3e), as it zipped along the boundary between an elongated, 4 km-long block of meteoric ice, and surrounding marine ice. At the same time, a noticeable reduction in the far-field stress can be seen in Figure 3e.

For both periods, we interpret the results as discontinuous (or episodic) rift propagation controlled by the heterogeneous structure of the ice shelf. The relatively stagnant phases occurred when the fracture tips encountered zones of inhomogeneous ice with different mechanical properties (King et al., 2018), causing a temporary fracture arrest and allowing the build-up of the far-field tensile stress. Once the tension caused favourable conditions for rift propagation, a phase of rapid lengthening and

5   stress release followed. Results suggest that discontinuous rift propagation can be expected for all Antarctic ice shelves with heterogeneous properties, and unknown spatial variations in mechanical properties of the ice can lead to significant uncertainties in the timing of fracture initiation and the speed of rift propagation.

Our results show that by October 2018, the accumulated damage to the BIS had resulted in a significant loss of mechanical

10   coupling between the grounded ice at the MIR and the upstream ice shelf. This loss of mechanical contact provides an explanation for the overall reduction in compressive and tensile stress across the ice shelf (Figure 3b and e). In the near future, the details of the newly emerging ice shelf configuration will depend on the exact pathways of rift propagation (De Rydt et al., 2018, Hodgson et al., 2019). In the most likely scenario, the ice shelf will approach its pre-2000 configuration with a (close-to) freely floating ice tongue, hence completing a 50-year calving cycle that started after the last calving event in the 1970s.

15   However, the potentially complex interaction between two active rifts, and the nascent loss of the largest area of ice since records began in 1915, result in an uncertain future for the ice shelf.

6 Transient simulations of ice dynamics changes

Based on the available observational data, we identified two characteristic phases in the life cycle of the BIS: ice-shelf growth causing stress accumulation and slow-down, followed by rift formation causing stress release and speed-up. Both phases are

20   thought to be representative for many present-day buttressed ice shelves in Antarctica, and it is imperative that time-evolving (transient) numerical simulations of ice flow are able to represent both phases with confidence in order to make robust projections of Antarctica's future ice-shelf extent and flow.

In order to verify the capability of state-of-the-art ice flow models to reproduce observed changes in flow speed of the BIS,

25   we used the ice flow model Úa in a transient mode. The model simulation was started from the 01/01/1999 ice shelf configuration, with estimates of the rate factor $A(\vec{x})$ obtained from the corresponding inverse step to ensure an optimal fit between the initial model velocities and observations, as shown in Figure 4a. The initial ice draft did not make contact with the seabed at the MIR, but in order to allow the ice front to advance beyond its initial location and establish grounding at the MIR, two modifications were added to the model configuration: 1) The unknown shape of the bedrock at the MIR was

30   prescribed by a 3D Gaussian bump with peak elevation of 130 m below sea level, i.e. between 10 and 50 m above the local ice draft. 2) The computational domain was artificially extruded into the open ocean towards the north of the BIS, and covered with a thin layer of ice with a uniform thickness of 1 m and a spatially constant rate factor $A = 3.5 \times 10^{-25}\,\mathrm{s}^{-1}\,\mathrm{Pa}^{-3}$, corresponding

27

to ice at -10 °C (Cuffey and Paterson, 2010). The thin ice cover, which is masked in Figure 4, has limited effect on the initial dynamics of the ice shelf. A fully implicit time integration with streamline upwind Petrov-Galerkin method and stabilization (SUPG) was used, and the ice front was found to advance with limited diffusion or spurious oscillations.

5   After 10 years of transient evolution, during which the ice shelf geometry, ice thickness and flow velocities were allowed to freely evolve, the magnitude and spatial distribution of simulated changes in surface speed remained largely consistent with observations (Figure 4b). In particular, growth of the ice shelf generated an expanding area of ice-bed contact at the MIR and the increasing amount of basal traction, parameterized by a Weertman sliding law as described in section 4, caused a slow-down of the ice shelf by up to 1.2 m/d, both in the observational data set and the numerical simulations. The striking similarities

10   between the observed and modelled patterns of change between 1999 and 2010 provide a powerful validation for the predictive skill of Úa (and, consequently, for models with a comparative representation of ice dynamics) over the given time period. To our knowledge, this is the first successful hindcast of a numerical ice-flow model against observed transient changes in ice-flow velocities of an Antarctic ice shelf.

15   It is important to note that throughout the simulation, the initial spatial distribution of the rate factor was kept fixed in space, and any changes in ice flow that could result from the advection of A with the ice, or changes due to temperature variations and fracture, were ignored. This approach is commonly used in transient ice flow modelling (see e.g. Arthern and Williams, 2017, Yu et al., 2018, Martin et al., 2019 for recent studies), and is based on the assumption that spatiotemporal changes in A are sufficiently slow and do not significantly affect the solution on the timescales under consideration. The agreement between

20   observed and modelled flow changes for the BIS (Figure 4b) demonstrates that, at least between 1999 and 2010, potential changes in A are not required to explain the observed slow-down of the ice shelf, and the large-scale dynamics of the BIS is, to first-order, controlled by the amount of pinning at the MIR.

However, following the re-activation of Chasm 1 in 2012 and the formation of the Halloween Crack in 2016, the assumption

25   of a constant rate factor A breaks down. In order to capture the dynamical impact of rift formation, areas of soft ice or discontinuities in the mesh need to be introduced (see Appendices A and B for more details). Both methods provide an effective way of describing the initiation and propagation of fractures, often referred to as 'damage' (e.g. Borstad et al., 2012) or a 'calving law'.

30   In order to quantify the errors in numerical simulations caused by the absence of a suitable dynamical description of fractures in our model, we continued transient simulation with Úa with constant A for another 8 years (2011 to 2018), and compared model output to direct observations of the surface velocity in October 2018. Between 2011 and 2018, Chasm 1 and the Halloween Crack propagated as shown in Figure 4c, and caused a loss of buttressing and widespread speed-up of the ice shelf. However, numerical projections of the flow remained largely constant or slightly decreased over this period (Figure 4c). As a

28

consequence, model simulations in the absence of a suitable fracture model underestimated the flow speed upstream of Chasm 1 by up to 25%, and by 100% on sections that became partly disconnected from the main ice shelf, over a period of only 7 years. The use of a constant rate factor therefore requires careful consideration and, at least for the BIS, a suitable treatment of fractures is needed to capture dynamical changes during a full cycle of growth and collapse.

5

7 Concluding remarks

Our results, based on observations and numerical modelling, demonstrate how ice shelves that are dynamically constrained by local pinning points, such as the Brunt Ice Shelf, can experience significant changes in internal stress over decadal timescales, due to their naturally evolving geometry. Favourable conditions for rifting can develop far upstream of the ice front, which makes these ice shelves particularly vulnerable to a loss of structural integrity. In combination with an often-heterogeneous internal ice structure, the mechanical conditions that control rift formation and propagation are complex and are not generally exploited in present-day ice flow models, despite recent progress (Levermann et al., 2012; Borstad et al., 2012). Existing calving criteria based on a maximum ice thickness, such as the marine ice-cliff instability mechanism (De Conto and Pollard, 2016), remain controversial (Edwards et al., 2019) and might not be directly relevant for thin floating areas such as the Brunt Ice Sheld. Other commonly-used calving laws based on minimum ice thickness criteria discard variations in mechanical properties of the ice, and are independent of internal stress. Existing theories for the vertical propagation of surface and basal crevasses (Hughes, 1983, van der Veen, 1998a, 1998b), often linked to surface hydrology (Scambos et al, 2000, Scambos et al., 2009, Nick et al., 2013), do not generally include criteria for the initiation and horizontal propagation of full-depth rifts. Glaciological changes on the Brunt Ice Shelf have unequivocally demonstrated that detailed knowledge about local pinning points, the internal structure of the ice shelf and a comprehensive treatment of fracture mechanics in ice flow models, are equally essential to capture rapid and large-scale changes in ice shelf dynamics, and thereby incorporate the critical role of ice shelves as a buffer against future mass loss from the Antarctic Ice Sheet.

Code and data availability

Author contributions

J.D.R. and G.H.G. designed and initiated the project; T.N. and J.W. processed the satellite data; G.H.G. and J.D.R. were responsible for in-situ data collection, processing and quality control; J.D.R. performed the model simulations, carried out the data analysis and prepared the figures and manuscript; G.H.G., T.N. and J.W. reviewed and edited the manuscript.

5 **Competing interests**

The authors declare no competing interests.

References

Anderson, R., Jones, D. H. and Gudmundsson, G. H.: Halley Research Station, Antarctica: calving risks and monitoring strategies, Natural Hazards and Earth System Sciences, 14, 917–927, 2014.

15 Arndt, J. E., Larter, R. D., Friedl, P. , Gohl, K., Hoppner, K. and the Science Team of Expedition PS104: Bathymetric controls on calving processes at Pine Island Glacier , The Cryosphere, 12(6), pp. 2039–2050, 2018.

Arthern, R. J., and Williams, C. R.: The sensitivity of West Antarctica to the submarine melting feedback, Geophysical Research Letters, 44, 2352– 2359, 2017.

20

Bassis, J. N., Coleman, R., Fricker, H. A. and Minster, J. B.: Episodic propagation of a rift on the Amery Ice Shelf, East Antarctica, Geophysical Research Letters, 32, 2005.

Bassis, J. N., Fricker, H. A., Coleman, R. and Minster, J.-B.: An investigation into the forces that drive ice-shelf rift
25 propagation on the Amery Ice Shelf, East Antarctica, Journal of Glaciology, 54, 17–27, 2008.

Berger, S., Favier, L., Drews, R., Derwael, J.-J., and Pattyn, F.: The control of an uncharted pinning point on the flow of an Antarctic ice shelf, Journal of Glaciology, 62(231), 37-45, doi:10.1017/jog.2016, 2016.

Bindschadler, R., Choi, H., Wichlacz, A., Bingham, R., Bohlander, J., Brunt, K., Corr, H., Drews, R., Fricker, H., Hall, M., Hindmarsh, R., Kohler, J., Padman, L., Rack, W., Rotschky, G., Urbini, S., Vornberger, P., and N. Young, N..: Getting around Antarctica: new high-resolution mappings of the grounded and freely-floating boundaries of the Antarctic ice sheet created for the International Polar Year, The Cryosphere 5, 569–588, 2011.

Borstad, C. P., Khazendar, A., Larour, E., Morlighem, M., Rignot, E., Schodlok, M. P. and Seroussi H.: A damage mechanics assessment of the Larsen B ice shelf prior to collapse: Toward a physically-based calving law, Geophysical Research Letters, 39, L18502, 2012.

Borstad, C. P., Rignot, E., Mouginot, J., and Schodlok, M. P.: Creep deformation and buttressing capacity of damaged ice shelves: theory and application to Larsen C ice shelf, The Cryosphere, 7, 1931–1947, doi:10.5194/tc-7-1931-2013, 2013.

Borstad, C., McGrath, D. and Pope, A.: Fracture propagation and stability of ice shelves governed by ice shelf heterogeneity, Geophysical Research Letters, 44, 4186–4194, 2017.

Cuffey, K. and Paterson, W.: The physics of glaciers (Academic Press, 2010), fourth edn.

De Conto, R. M. and Pollard, D.: Contribution of Antarctica to past and future sea-level rise, Nature, 531, 591–597, 2016.

De Rydt, J., Gudmundsson, G. H., Nagler, T., Wuite, J. and King, E. C.: Recent rift formation and impact on the structural integrity of the Brunt Ice Shelf, East Antarctica, The Cryosphere, 12, 505–520, 2018.

Depoorter, M. A., Bamber, J.L., Griggs, J.A., Lenaerts, J.T.M., Ligtenberg, S.R.M., van den Broeke, M.R. and Moholdt, G.: Calving fluxes and basal melt rates of Antarctic ice shelves, Nature, 502, 89–92, 2013.

Doake, C. S. M., Corr, H. F. J., Rott, H., Skvarca, P. and Young, N. W.: Breakup and conditions for stability of the northern Larsen Ice Shelf, Antarctica, Nature, 391, 778–780, 1998.

Dupont, T. K. and Alley, R. B.: Assessment of the importance of ice-shelf buttressing to ice-sheet flow, Geophysical Research Letters, 32, 2005.

Edwards, T. L., Brandon M. A., Durand, G., Edwards, N. R., Golledge, N. R., Holden, P. B., Nias, I. J., Payne, A. J., Ritz, C. and Wernecke, A.: Revisiting Antarctic ice loss due to marine ice-cliff instability, Nature, 566, 58–64, 2019.

Engwirda, D.: Locally-optimal Delaunay-refinement and optimisation-based mesh generation. Ph.D. thesis, School of Mathematics and Statistics, The University of Sydney, 2014.

5   Favier, L., Pattyn, F., Berger, S., and Drews, R.: Dynamic influence of pinning points on marine ice-sheet stability: a numerical study in Dronning Maud Land, East Antarctica, The Cryosphere, 10, 2623-2635, https://doi.org/10.5194/tc-10-2623-2016, 2016.

Flament, T. and Rémy, F.: Dynamic thinning of Antarctic glaciers from along-track repeat radar altimetry, Journal of
10   Glaciology, 58, 830–840, 2012.

Fretwell, P., Pritchard, H. D., Vaughan, D. G., Bamber, J. L., Barrand, N. E., Bell, R., Bianchi, C., Bingham, R. G., Blankenship, D. D., Casassa, G., Catania, G., Callens, D., Conway, H., Cook, A. J., Corr, H. F. J., Damaske, D., Damm, V., Ferraccioli, F., Forsberg, R., Fujita, S., Gim, Y., Gogineni, P., Griggs, J. A., Hindmarsh, R. C. A., Holmlund, P., Holt,
15   J. W., Jacobel, R. W., Jenkins, A., Jokat, W., Jordan, T., King, E. C., Kohler, J., Krabill, W., Riger-Kusk, M., Langley, K. A., Leitchenkov, G., Leuschen, C., Luyendyk, B. P., Matsuoka, K., Mouginot, J., Nitsche, F. O., Nogi, Y., Nost, O. A., Popov, S. V., Rignot, E., Rippin, D. M., Rivera, A., Roberts, J., Ross, N., Siegert, M. J., Smith, A. M., Steinhage, D., Studinger, M., Sun, B., Tinto, B. K., Welch, B. C., Wilson, D., Young, D. A., Xiangbin, C. and Zirizzotti, A Bedmap2: improved ice bed, surface and thickness datasets for Antarctica, The Cryosphere 7, 375–393, 2013.
20
Fricker, H. A., Young, N. W., Allison, I. and Coleman, R.: Iceberg calving from the Amery Ice Shelf, East Antarctica, Annals of Glaciology, 34, 2002.

Fürst, J. J., Durand, G., Gillet-Chaulet, F., Tavard, L., Rankl, M., Braun, M. and Gagliardini, G. The safety band of
25   Antarctic ice shelves. Nature Climate Change 6, 479–782, 2016.

Gudmundsson, G. H., De Rydt, J. and Nagler, T.: Five decades of strong temporal variability in the flow of Brunt Ice Shelf, Antarctica, Journal of Glaciology, 63, 164–175, 2017.

30   Gudmundsson, G. H., Krug, J., Durand, G., Favier, L. and Gagliardini, O.: The stability of grounding lines on retrograde slopes, The Cryosphere, 6, 1497–1505, 2012.

Hodgson, D. A., Jordan, T. A., De Rydt, J., Fretwell, P. T., Seddon, S. A., Becker, D., Hogan, K. A., Smith, A. M., and Vaughan, D. G.: Past and future dynamics of the Brunt Ice Shelf from seabed bathymetry and ice shelf geometry, The Cryosphere, 13, 545-556, 2019.

5   Hogg, A. E. and Gudmundsson, G. H.: Impacts of the Larsen-C ice shelf calving event, Nature Climate Change, 7, 540, 2017.

Howat, I. M., Porter, C., Smith, B. E., Noh, M.-J. and Morin, P.: The reference elevation model of Antarctica. The Cryosphere, 13, 665-674, 2019.

10

Hughes, T.: On the Disintegration of Ice Shelves: The Role of Fracture, Journal of Glaciology, 29, 98–117, 1983.

Joughin, I., and MacAyeal, D. R.: Calving of large tabular icebergs from ice˘ shelf rift systems. Geophysical Research Letters, 32, 2005.

15

Khazendar, A., Rignot, E. and Larour, E.: Roles of marine ice, rheology, and fracture in the flow and stability of the Brunt/Stancomb-Wills Ice Shelf, Journal of Geophysical Research: Earth Surface, 114, 2009.

King, E. C., De Rydt, J. and Gudmundsson, G. H.: The internal structure of the Brunt Ice Shelf from ice-penetrating radar
20   analysis and implications for ice shelf fracture, The Cryosphere, 12, 3361–3372, 2018.

Konrad, H., Gilbert, L., Cornford, S.L., Payne, A., Hogg, A., Muir, A. and Shepherd, A..: Uneven onset and pace of ice-dynamical imbalance in the Amundsen Sea Embayment, West Antarctica, Geophysical Research Letters, 44, 910–918, 2016.

25

Larour, E., Rignot, E., and Aubry, D.: Modelling of rift propagation on Ronne Ice Shelf, Antarctica, and sensitivity to climate change, Geophysical Research Letters, 31, L16404, 2004.

Larour, E., Rignot, E., Joughin, I., and Aubry, D.: Rheology of the Ronne Ice Shelf, Antarctica, inferred from satellite
30   radar interferometry data using an inverse control method, Geophysical Research Letters, 32, L05503, doi:10.1029/2004GL021693, 2005.

Levermann, A., Albrecht, T., Winkelmann, R., Martin, M. A., Haseloff, M., and Joughin, I.: Kinematic first-order calving law implies potential for abrupt ice-shelf retreat, The Cryosphere, 6, 273-286, https://doi.org/10.5194/tc-6-273-2012, 2012.

Lipovsky, B. P.: Ice Shelf Rift Propagation and the Mechanics of Wave-Induced Fracture, Journal of Geophysical Research: Oceans, 123, 4014–4033, 2018a.

MacAyeal, D.: A tutorial on the use of control methods in ice-sheet modelling, Journal of Glaciology, 39(131), 91-98, 1993

Martin, D. F., Cornford, S. L., and Payne, A. J.: Millennial-scale vulnerability of the Antarctic Ice Sheet to regional ice shelf collapse. Geophysical Research Letters, 46, 1467– 1475, 2019.

Matsuoka, K., Hindmarsh, R. C. A., Moholdt, G., Bentley, M. J., Pritchard, H. D., Brown, J., Conway, H., Drews, R., Durand, G., Goldberg, D., Hattermann, T., Kingslake, J., Lenaerts, J. T. M., Martín, C., Mulvaney, R., Nicholls, K. W., Pattyn, F., Ross, N., Scambos, T., and Whitehouse, P. L.: Antarctic ice rises and rumples: Their properties and significance for ice-sheet dynamics and evolution, Earth-Science Reviews, 150, 724-745, https://doi.org/10.1016/j.earscirev.2015.09.004, 2015.

Mouginot, J., Rignot, E., Scheuchl, B. and Millan, R.: Comprehensive annual ice sheet velocity mapping using Landsat-8, Sentinel-1, and RADARSAT-2 data, Remote Sensing, 9, 2017.

Nagler, T., Rott, H., Hetzenecker, M., Wuite, J. and Potin, P.: The sentinel-1 mission: New opportunities for ice sheet observations, Remote Sensing 7, 9371–9389, 2015.

Nicholls, K. W., Østerhus, S., Makinson, K., Gammelsrød, T. and Fahrbach, E.: Ice-ocean processes over the continental shelf of the southern Weddell Sea, Antarctica: A review, Reviews of Geophysics, 47, 2009.

Nick F. M., Vieli, A., Langer Andersen, M., Joughin, I., Payne, A., Edwards, T. L., Pattyn, F. and van de Wal, R. S. W.: Future sea-level rise from Greenland's main outlet glaciers in a warming climate, Nature, 497, 235–238, 2013.

Paolo, F. S., Fricker, H. A. and Padman, L.: Volume loss from Antarctic ice shelves is accelerating, Science, 348, 327–331, 2015.

34

Pritchard, H. D., Arthern, R. J., Vaughan, D. G. and Edwards, L. A.: Extensive dynamic thinning on the margins of the Greenland and Antarctic ice sheets, Nature, 461, 971–975, 2009.

Reeh, N.: On the calving of ice from floating glaciers and ice shelves, Journal of Glaciology, 7, 215–232, 1968.

Reese, R., Winkelmann, R. and Gudmundsson, G. H.: Grounding-line flux formula applied as a flux condition in numerical simulations fails for buttressed Antarctic ice streams, The Cryosphere 12, 3229–3242, 2018.

Rignot, E., Casassa, G., Gogineni, P., Krabill, W., Rivera, A. and Thomas, R.: Accelerated ice discharge from the Antarctic Peninsula following the collapse of Larsen B ice shelf, Geophys. Res. Lett., 31, L18401, 2004.

Rist, M. A., Sammonds, P. R., Oerter, H. and Doake, C. S. M.: Fracture of Antarctic shelfice, Journal of Geophysical Research: Solid Earth, 107, 2002.

Rott, H., Müller, F., Nagler, T. and Floricioiu, D.: The imbalance of glaciers after disintegration of Larsen-B ice shelf, Antarctic Peninsula, The Cryosphere, 5, 125–134, 2011.

Scambos, T. A., Bohlander, J. A., Shuman, C. A. and Skvarca, P.: Glacier acceleration and thinning after ice shelf collapse in the Larsen B embayment, Antarctica, Geophysical Research Letters, 31, 2004.

Scambos, T. A., Hulbe, C., Fahnestock, M. and Bohlander, J.: The link between climate warming and break-up of ice shelves in the Antarctic Peninsula, Journal of Glaciology, 46, 516–530, 2000.

Scambos, T., Fricker, H. A., Liu, C.-C., Bohlander, J., Fastook, J., Sargent, A., Massom, R. and Wu, A.-M.f: Ice shelf disintegration by plate bending and hydro-fracture: Satellite observations and model results of the 2008 Wilkins ice shelf break-ups, Earth and Planetary Science Letters, 280, 51 − 60, 2009.

Simmons, D. and Rouse, J.: Accelerating flow of the Brunt Ice Shelf, Antarctica, Journal of Glaciology, 30, 377–380, 1984.

Simmons, D.: Flow of the Brunt Ice Shelf, Antarctica, Derived from Landsat Images, 1974–85, Journal of Glaciology, 32, 252–254, 1986.

Slater, T., Shepherd, A., McMillan, M., Muir, A., Gilbert, L., Hogg, A. E., Konrad, H. and Parrinello, T.: A new digital elevation model of Antarctica derived from CryoSat-2 altimetry, The Cryosphere, 12, 1551–1562, 2018.

Thomas, R. H.: The creep of ice shelves: Interpretation of observed behaviour, Journal of Glaciology, 12, 55–70, 1973.

van der Veen, C.: Fracture mechanics approach to penetration of surface crevasses on glaciers, Cold Regions Science and Technology, 27, 31 – 47, 1998a.

van der Veen, C.: Fracture mechanics approach to penetration of bottom crevasses on glaciers, Cold Regions Science and Technology, 27, 213 – 223, 1998b.

Walker, C., Bassis, J., Fricker, H., and Czerwinski, R.: Observations of interannual and spatial variability in rift propagation in the Amery Ice Shelf, Antarctica, 2002–14. Journal of Glaciology, 61(226), 243-252. doi:10.3189/2015JoG14J151, 2015.

Yu, H., Rignot, E., Seroussi, H. and Morlighem, M.: Retreat of Thwaites Glacier, West Antarctica, over the next 100 years using various ice flow models, ice shelf melt scenarios and basal friction laws, The Cryosphere, 12, 3861-3876, 2018.

Figure 1: Map of the Brunt Ice Shelf with inset showing its location in relation to the Antarctic continent (Howat et al., 2019). Panel a shows the ice shelf in 2010, prior to rifting. The grounding lines (solid black lines, (Bindschadler et al., 2011)), open ocean shaded in blue, and surface velocities from the MEaSUREs 2010-2011 annual Antarctic velocity map (white arrows, (Mouginot et al., 2017)), are overlain on a Landsat-7 panchromatic image collected on 4 January 2010. All velocity maps in this study have been cross-calibrated to data from a network of up to 15 in situ GPS stations. The configuration of the network in 2010 is shown by the yellow dots, with corresponding velocity arrows in black. Panel b shows the extent of two active rifts – 'Chasm 1' and the 'Halloween Crack' – in October 2018, with cyan arrows indicating their direction of propagation. Black arrows represent velocity anomalies between 2010, prior to rift initiation, and February 2018 (Sentinel-1 data), showing a dramatic increase in flow as a result of ice-shelf rifting. Blue-to-red colors illustrate the corresponding change in surface speed. Ice front locations in 1978, 2010 and 2018 are shown for reference.
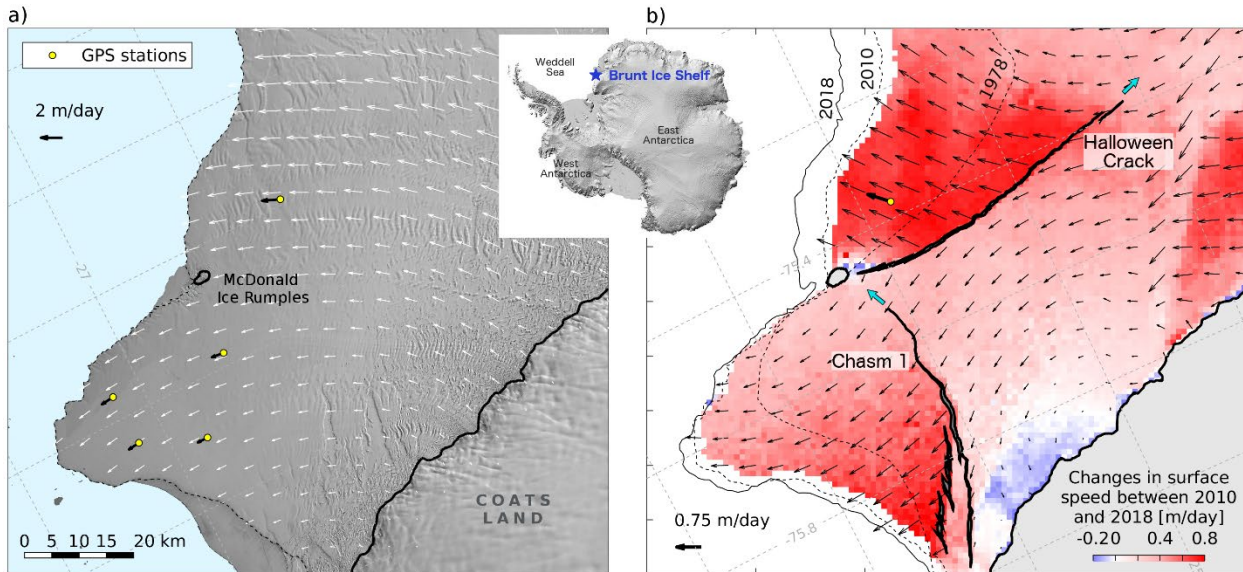
Figure 2: Temporal evolution of principal deviatoric stress components (black arrows for extension, red arrows for compression) and maximum deviatoric stress amplitude (colours) as the Brunt Ice Shelf re-grounds at the McDonald Ice Rumples (panel b). The blue marker in panel c indicates the historical tip of Chasm 1, which corresponds to the onset location of rift propagation in December 2012. The blue marker in the panel d shows the onset location of the Halloween Crack on 4 October 2016. Panels are dated with the time stamp of the corresponding surface velocity used in the diagnostic calculation of the stress field (Table 1). Black boxes in panel d indicate the geographical extent of panels in Figure 3.
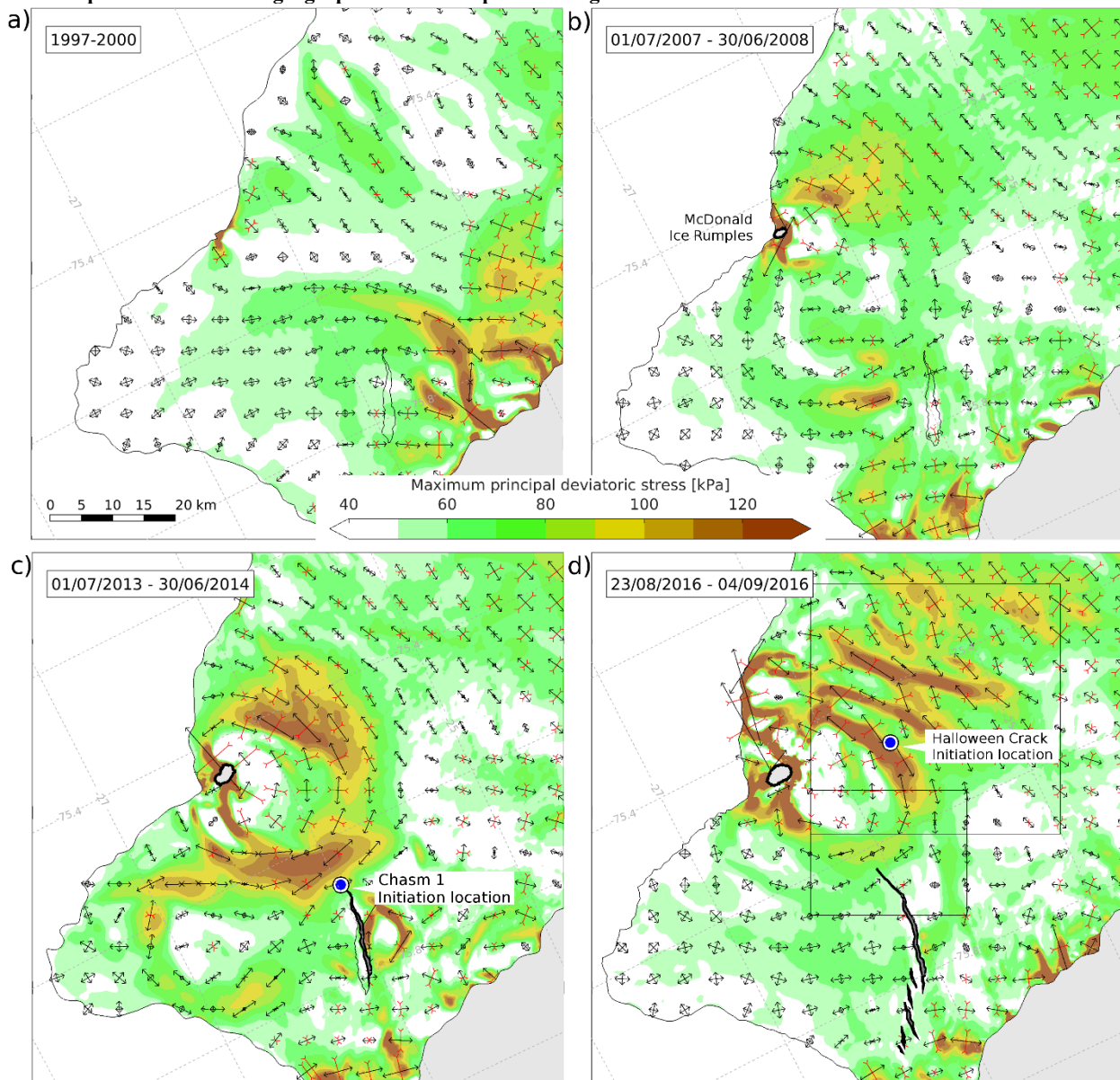
Figure 3: Build-up and reduction in tensile stress during discontinuous rift propagation. Top row: the Halloween Crack remained stagnant for most of November 2016 resulting in the localized accumulation of stress, before propagating 11 km in December 2016 and causing a significant release of stress. Bottom row: Chasm 1 lengthened by only 500 m in 2016 compared to 1.5 km/yr in preceding years, and by January 2017, a zone of high tensile stress developed ahead of the rift tip (panel c). This zone intensified by May 2017 (panel d) and tension dissipated by October 2017 (panel e), following a rapid progression by 4.5 km. For reference, the blue markers indicate the location of rift initiation as in Figure 2, and the dashed contours panels b and e correspond to the stresses before propagation.
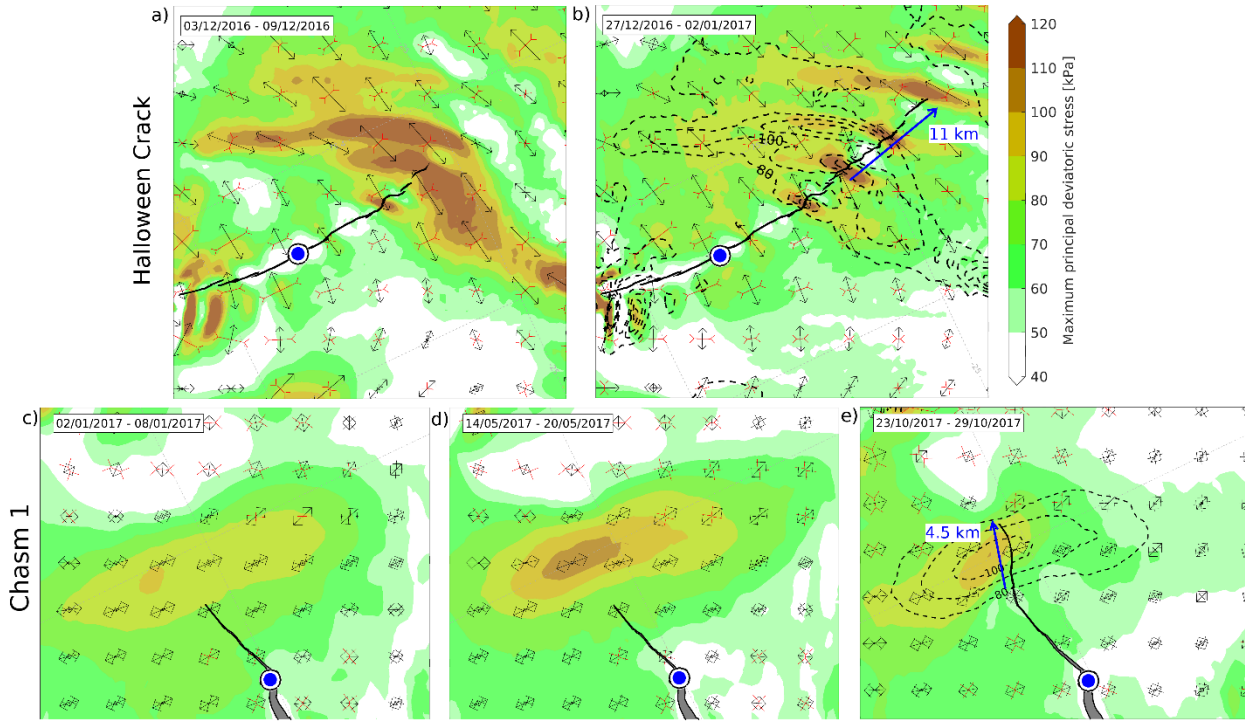
Figure 4: Comparison between observed (left column) and modelled (right column) surface speed of the Brunt Ice Shelf between 2000 and 2018. The 2000 ice front location is shown by the dashed lines and the extent of the McDonald Ice Rumples is shaded in grey. Observations and model simulations broadly agree in 2000, and both show a significant slow-down between 2000 and 2011due to increasing contact between the ice-shelf draft and a seabed shoal at the McDonald Ice Rumples. However, observations and model simulations strongly diverge after the formation and propagation of Chasm 1 (2012) and the Halloween Crack (2016). This difference is because Chasm1 is not generated within the numerical model due to the model's lack of a fracture mechanical component. This situation is typical for current generation of large-scale ice shelf models. Here, these differences lead to ice flow speed being underestimated by more than 1 m/day (or up to 100%) at the end of a transient run over less than a decade.
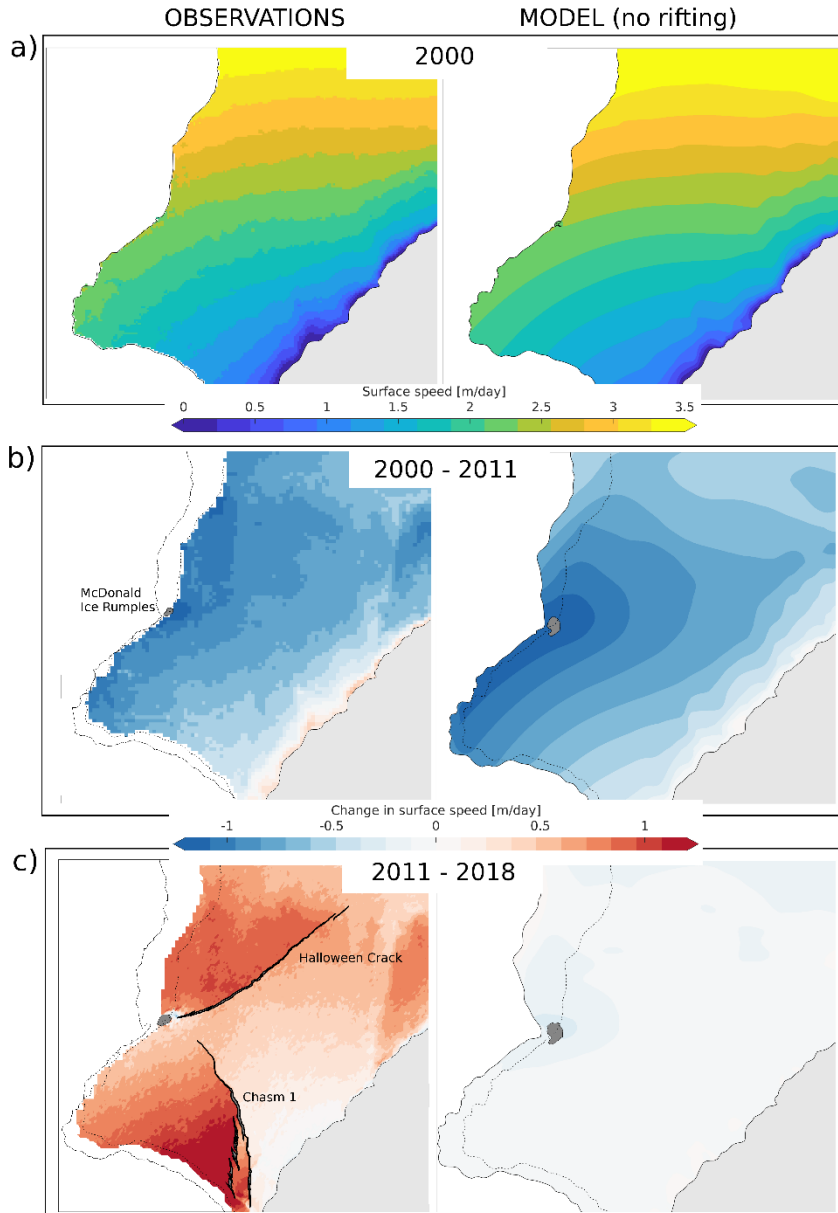
40

Table 1. Data sources and corresponding timestamps used for the stress calculations. The effective timestamp in the first column corresponds to the middle of the velocity feature tracking window, and WorldView-2 surface elevations were shifted to the corresponding effective time stamp.

Effective time stamp	Surface DEM	Surface velocity	Ice front location
01/01/1999	Bedmap 2 *(Fretwell et al., 2013)*	RADARSAT1 *(Khazendar et al., 2009)* 1997-2001	Landsat 7 14/02/2001
01/01/2008	WorldView-2	MEaSUREs *(Mouginot et al., 2017)* 01/07/2007 – 30/06/2008	Landsat 7 18/12/2007
01/01/2014	WorldView-2	MEaSUREs 01/07/2013 – 30/06/2014	Landsat 7 04/01/2014
29/08/2016	WorldView-2	Sentinel-1A/B 23/08/2016 – 04/09/2016	Landsat 8 29/09/2016
06/12/2016	WorldView-2	Sentinel-1A/B 03/12/2016 – 09/12/2016	Landsat 8 09/12/2016
30/12/2016	WorldView-2	Sentinel-1A/B 27/12/2016 – 02/01/2017	Landsat 8 01/01/2017
06/01/2017	WorldView-2	Sentinel-1A/B 02/01/2017 – 08/01/2017	Landsat 8 01/01/2017
17/05/2017	WorldView-2	Sentinel-1A/B 14/05/2017 – 20/05/2017	Landsat 8 15/03/2017
27/10/2017	WorldView-2	Sentinel-1A/B 27/10/2017 – 29/10/2017	Landsat 8 25/10/2017

5

Appendix A. Inverse method and results

A.1 Model domain and computational mesh

The computational domain includes the Brunt Ice Shelf and Stancomb Wills Glacier Tongue, analogous to Gudmundsson et al, 2017 and De Rydt et al., 2018, in order to fully account for the weak mechanical coupling between both ice shelves. Only results for the Brunt Ice Shelf are presented here. The ice front location and extent of the McDonald Ice Rumples (MIR) for each ice-shelf configuration were outlined from satellite images, as specified in Section 3 and Table 1. The location of the southern grounding line, which marks the edge between the ice shelf and the adjacent Coats Land (Figure 1), was obtained from (Bindschadler et al., 2011). The computational domain was truncated at the grounding line, and Dirichlet boundary conditions were used to impose the velocities along this edge.

For each ice shelf geometry, an unstructured computational mesh was generated using MESH2D (Engwirda, 2014), and consisted of linear elements with 6 integration points and a mean nodal spacing of 325 m with local mesh refinement down to 100 m nodal spacing around the MIR. All results presented in the main part of the paper were obtained for a continuous mesh, and rifts were treated as 'soft ice' with a finite ice thickness. Alternatively, known rifts can be outlined from satellite imagery and cut out of the computational domain. The resulting holes in the mesh are filled with water, and have ocean pressure acting on the edges. The differences between both methods are discussed in more detail in Appendix B.

A.2 Inverse method

An adjoint method was used to obtain optimal estimates of the rate factor $A(\vec{x})$ for given surface velocities $u_{observed}$, ice thickness and ice shelf geometry. The cost function J was defined as

(A1) $\quad J = J_{misfit} + J_{regularization}$

$$= \frac{1}{2\mathcal{A}} \iint dx \; (u_{model} - u_{observed})^2/\varepsilon^2 + \frac{1}{2\mathcal{A}} \iint dx \; \left(\gamma_s^2 (\nabla \log_{10}(A/\hat{A}))^2 + \left(\log_{10}(A/\hat{A}) \right)^2 \right),$$

with $\mathcal{A} = \iint dx$, ε the data errors and $\hat{A} = 1.146 \times 10^{-8}$ kPa^{-3}yr^{-1} the a priori value of the rate factor, which corresponds to a uniform ice temperature of -10°C. The adjoint method calculates $A(\vec{x})$ as a solution of the minimization problem d$_A J$=0 using an iterative optimization algorithm. The algorithm was stopped after 10,000 iterations, when fractional changes to the cost function were less than 10^{-5}. An optimal value for the Tikhonov regularization multiplier γ_s in the cost function was determined using an L-curve approach. Figure A1 shows that $\hat{\gamma}_s$= 50,000 m produces the smallest misfit between observed and modelled surface velocities, whilst limiting the risk of overfitting, and is used throughout. The optimal value $\hat{\gamma}_s$, was found to be independent of the creep exponent n. Model inversions for different values of the creep exponent (n=2 and n=4) were carried out and results for the stress patterns (not shown) were found to be robust within the observational range of values for n (Cuffey and Paterson, 2010). Inversions for $10 \times \hat{\gamma}_s$ and $\hat{\gamma}_s/10$ (not shown) did not lead to any significant changes in the diagnostic stress patterns, and changes to the magnitude of the stress components were limited to less than 10%.

A.3 Examples of the rate factor $A(\vec{x})$

Figure A2 shows the estimated rate factor for two ice-shelf configurations: the left panel depicts $A(\vec{x})$ in 1999 before rift formation, whereas the right panel shows $A(\vec{x})$ in 2016 after the initiation of Chasm 1 and the Halloween Crack. Black contour

5   lines represent the corresponding 'ice temperature' in °C, as defined by Cuffey and Patterson, 2010:

(A2) $T = \left(-\frac{R}{Q_c}\log(A/A^*) + T^{*-1}\right)^{-1} - 273.15$

with A transformed to Pa^{-3}s^{-1} and $R = 8.314$ J mol^{-1} K^{-1}, $Q_c = 6e4$ J mol^{-1}, $A^* = 3.5e$-25 Pa^{-3} s^{-1}, $T^* = 263$. Values of A and T should be interpreted carefully, as they are vertically integrated quantities that do not only vary with ice temperature, but also include other effects such as ice rifting. This is obvious from the right hand panel, where consistently high values of A are

10 found along the rift trajectories and other crevassed areas such as the hinge zone immediately downstream of the grounding line. These areas of 'soft ice' accommodate the high strain rates or discontinuities in flow speed in those areas (compare to Figure 1b). At the MIR, extreme values of A can also result from fitting the data to the SSA flow approximation, which breaks down here because of the high vertical shear. In both panels of Figure A2, bands of stiffer (colder) ice are seen to follow flowlines from the grounding line to the ice front, and have previously been identified as bands of meteoric ice that originate

15 upstream of the grounding line, in contrast to the surrounding areas that predominantly consist of (warmer) marine ice (King et al., 2018). The recovery of the internal ice structure from A provides both an independent confirmation for the work of King et al., 2018, which was based on ground penetrating radar data, and additional support for the physical meaningfulness of A.

Appendix B. Representation of rifts in the computational domain.

20

Rifts that cut through the full thickness of the ice shelf can be (partially) filled with ice mélange, marine ice and snow. In some cases, the infill creates a mechanical coupling between vertical rift faces and provides tensile strength, as pointed out by Larour et al., 2004 for rifts in the Ronne Ice Shelf. The use of a continuous computational mesh in the inversion, which allows for non-zero ice thickness inside the rifts, seems most appropriate in this case. On the other hand, open water leads have routinely

25 been observed inside rapidly-evolving rifts such as Chasm 1 and the Halloween Crack, and opposite vertical rift faces are not or only partially connected. This justifies the representation of rifts as holes in the mesh, with ocean boundary conditions applied to the edges (the Hybrid and Water experiments in [Larour et al., 2004]). In case of the BIS, a numerical perturbation experiment by Gudmundsson et al., 2017 has shown that, prior to the reactivation of Chasm 1 in 2012, its mélange-filled area could be removed from the computational domain and replaced by open water without significant instantaneous impact on the

30 dynamics of the ice shelf.

In general, mélange thickness and areas of open water are not well constrained by observations, and the most appropriate choice of mesh type (continuous or with holes) is unclear. Here we demonstrate that, at least for Chasm 1 and the Halloween

Crack, the rate factor and diagnostic stress distribution are not critically dependent on this choice. In Figure B1 we compare values of the inferred rate factor A, the misfit between observations and model velocity, and the diagnostic principal stress components for the 06/12/2016 ice-shelf configuration. The left panels show results for a continuous mesh with a mélange thickness extrapolated from the thickness of neighbouring ice shelf areas. On the right, elements corresponding to rifts in the ice shelf were removed from the mesh, and ocean boundary conditions were imposed along the newly exposed faces.

For both limiting cases, the misfit between the modelled and observed flow speed is largely comparable (see insets in Figure B1) and relative errors are on the order of 5% or less. For a continuous mesh, high values of the rate factor along the rift trajectories represent weak ice, and reflect discontinuities in flow speed (or high strain rates) across the rifts, whereas such high values are mostly absent when rifts are represented by open water. In the latter case, any remnant areas of weak ice along the rifts are likely due to discrepancies between the outlines traced from visible satellite images and the true extent of the active rift (De Rydt et al., 2018). The principal stress directions are very similar in both cases, but with some notable differences in the magnitude of the maximum principal stress, in particular close to the tip of the Halloween Crack. The misfit between observed and modelled velocities in this area is larger in the open water case compared to the mélange case, causing a less accurate fit of the model to the observed strain rates, and a lower confidence in the derived stresses. All results in the main part of this paper were based on a continuous mesh.
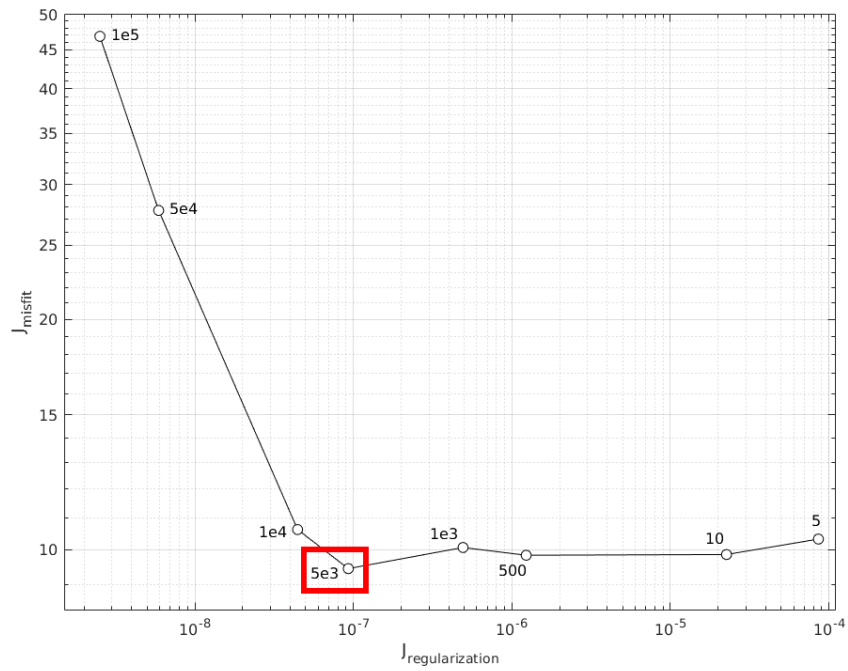
Figure A1. Example L-curve for the 01/01/2014 ice shelf configuration.
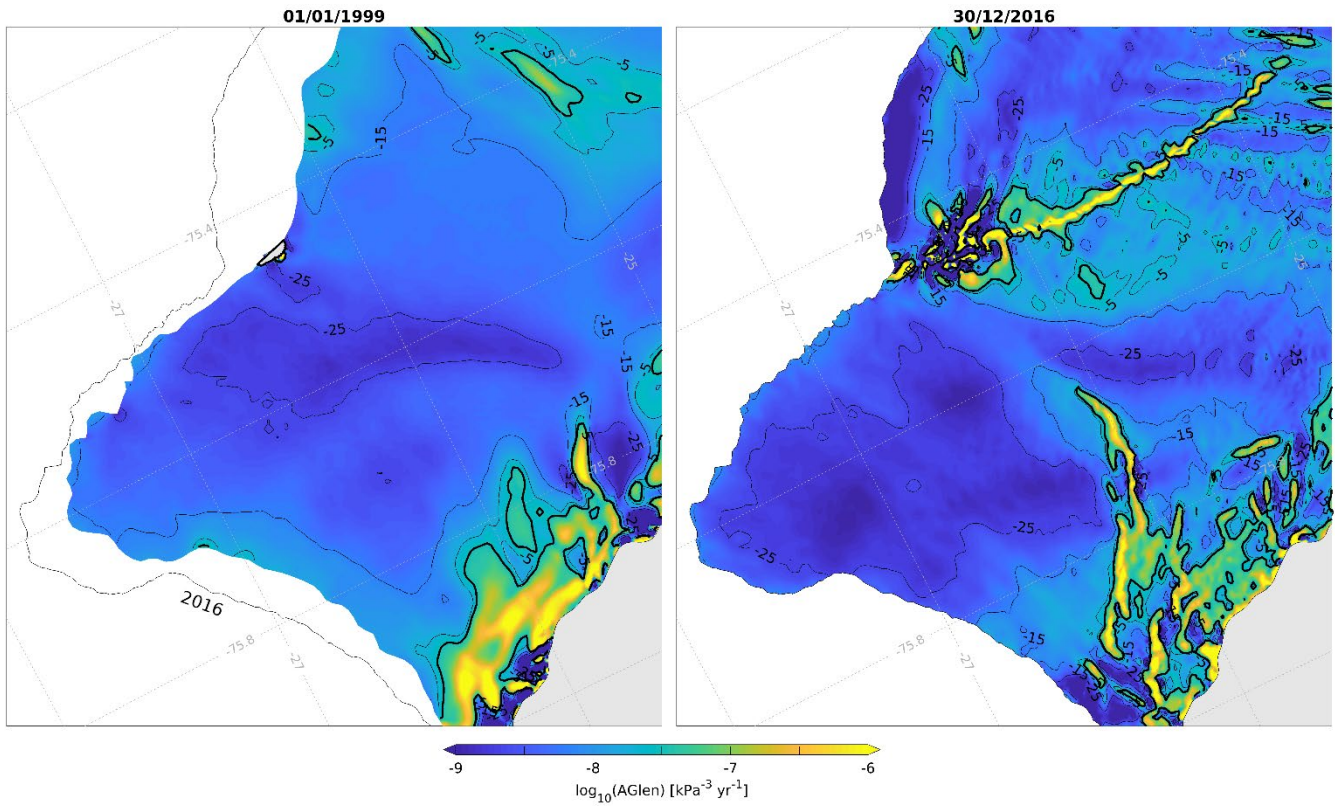
Figure A2. Examples of the rate factor *A* (colours) and associated 'ice temperatures' in °C (black contours) as calculated from eq. (A1) for the Brunt Ice Shelf prior to rift formation (01/01/1999, left panel) and after the initiation of Chasm 1 and the Halloween Crack (30/12/2016, right panel). Contours are plotted at 10 °C intervals and the zero degree contour is highlighted by the thicker line. The left panel shows the 2016 ice shelf extent for reference.
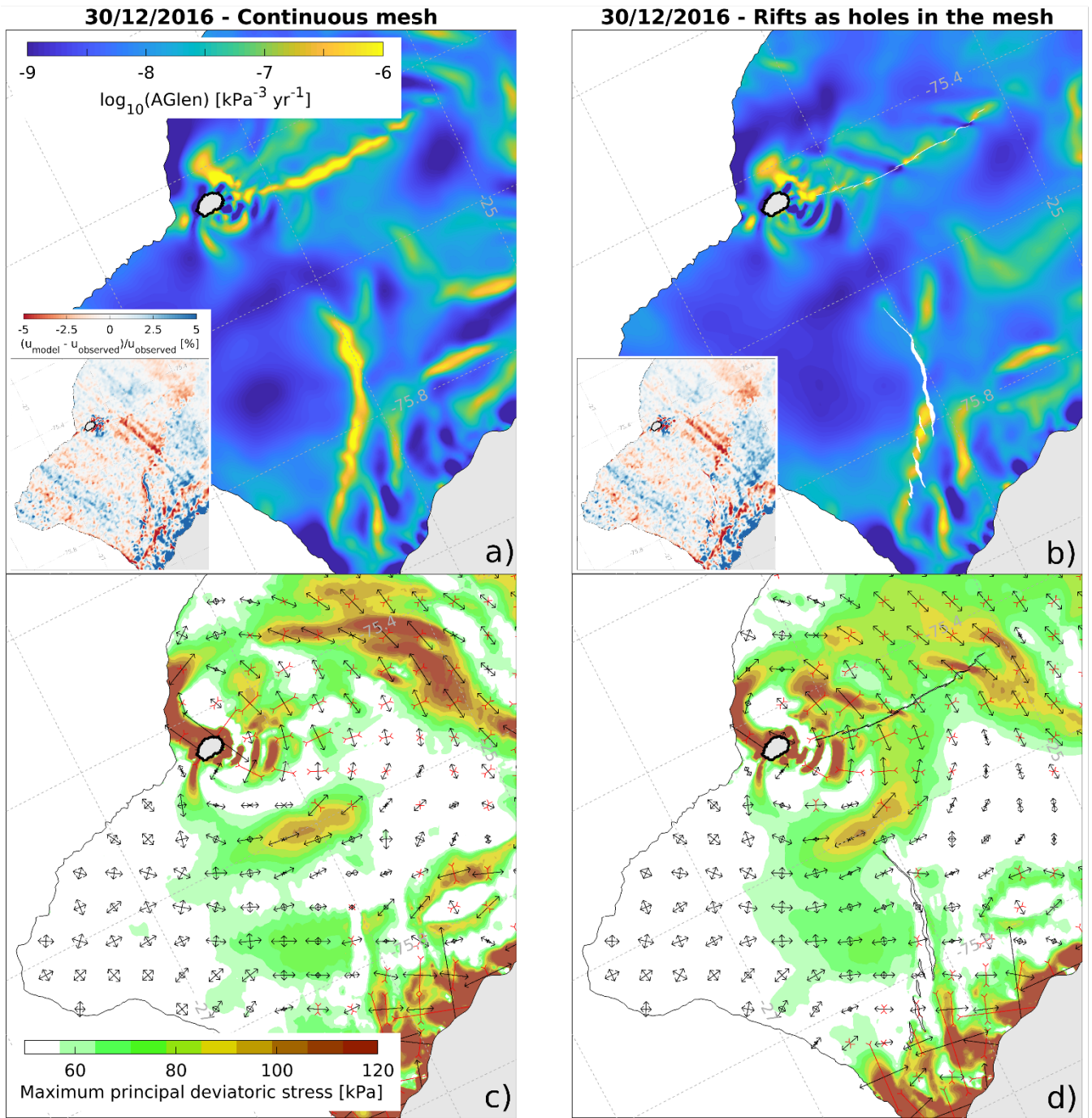
Figure B1. Spatial maps of the rate factor *A* (panels a and b) and diagnostic principal stresses (panels c and d) for the Brunt Ice Shelf on 06/12/2016. Results are based on identical input datasets, but for two different computational meshes: on the left (panels a and c), a continuous mesh was used and Chasm 1 and the Halloween Crack were filled with ice; on the right (panels b and d), rifts were represented as holes in the mesh with ocean boundary conditions.